Microbiome

RESEARCH Open Access

Vertically stratified methane, nitrogen and sulphur cycling and coupling mechanisms in mangrove sediment microbiomes

Lu Qian[1], Xiaoli Yu[1*], Hang Gu[1], Fei Liu[1], Yijun Fan[1], Cheng Wang[1], Qiang He[2], Yun Tian[3], Yisheng Peng[1], Longfei Shu[1], Shanquan Wang[1], Zhijian Huang[4], Qingyun Yan[1], Jianguo He[5], Guangli Liu[1], Qichao Tu[6] and Zhili He[1*]

Abstract

Background Mangrove ecosystems are considered as hot spots of biogeochemical cycling, yet the diversity, function and coupling mechanism of microbially driven biogeochemical cycling along the sediment depth of mangrove wetlands remain elusive. Here we investigated the vertical profile of methane (CH_4), nitrogen (N) and sulphur (S) cycling genes/pathways and their potential coupling mechanisms using metagenome sequencing approaches.

Results Our results showed that the metabolic pathways involved in CH_4, N and S cycling were mainly shaped by pH and acid volatile sulphide (AVS) along a sediment depth, and AVS was a critical electron donor impacting mangrove sediment S oxidation and denitrification. Gene families involved in S oxidation and denitrification significantly ($P < 0.05$) decreased along the sediment depth and could be coupled by S-driven denitrifiers, such as *Burkholderiaceae* and *Sulfurifustis* in the surface sediment (0–15 cm). Interestingly, all S-driven denitrifier metagenome-assembled genomes (MAGs) appeared to be incomplete denitrifiers with nitrate/nitrite/nitric oxide reductases (Nar/Nir/Nor) but without nitrous oxide reductase (Nos), suggesting such sulphide-utilizing groups might be an important contributor to N_2O production in the surface mangrove sediment. Gene families involved in methanogenesis and S reduction significantly ($P < 0.05$) increased along the sediment depth. Based on both network and MAG analyses, sulphate-reducing bacteria (SRB) might develop syntrophic relationships with anaerobic CH_4 oxidizers (ANMEs) by direct electron transfer or zero-valent sulphur, which would pull forward the co-existence of methanogens and SRB in the middle and deep layer sediments.

Conclusions In addition to offering a perspective on the vertical distribution of microbially driven CH_4, N and S cycling genes/pathways, this study emphasizes the important role of S-driven denitrifiers on N_2O emissions and various possible coupling mechanisms of ANMEs and SRB along the mangrove sediment depth. The exploration of potential coupling mechanisms provides novel insights into future synthetic microbial community construction and analysis. This study also has important implications for predicting ecosystem functions within the context of environmental and global change.

*Correspondence:
Xiaoli Yu
yuxli7@mail.sysu.edu.cn
Zhili He
hezhili@sml-zhuhai.cn
Full list of author information is available at the end of the article

Keywords Vertical distribution, Metagenome sequencing analysis, Mangrove sediment, Methane/nitrogen/sulphur cycling, Metagenome-assembled genome, Coupling mechanism

Background

Mangroves, one of the typical blue carbon ecosystems with the methane (CH_4) emission around 279.17 μmol m^{-2} day^{-1} on Earth [1], have tremendous ecological importance in the global carbon (C), nitrogen (N) and sulphur (S) cycles. The metabolic function of biogeochemical cycling processes is determined by biotic (e.g. microorganisms, microbial genes/pathways) and abiotic (e.g. pH, electron donors, electron acceptors) factors as well as their interactions [2–4]. Microbes are the engine that drives these biogeochemical processes and have profound effects on ecosystem functions [5], such as CH_4 emissions [6, 7], N transformation and removal [8, 9], and S reduction and oxidation [10, 11]. The 'hot spot' of microbially driven biogeochemical cycling could create an eco-buffer zone for shoreline protection, nutrient filtering, C storage and climate regulation [12].

Mangrove sediments form a dynamic environment and create an ideal natural gradient along the depth due to periodical tide movements, and fine gradients of physicochemical conditions, thus distinct microbial functions are observed at such land-sea interfaces [13–15]. For example, it was reported that denitrifiers had high activities and were responsible for major (~80%) N loss in the surface coastal sediment [16]. The high denitrification rate observed in the presence of O_2 could be explained by the adaptation of denitrifying bacteria to tidally induced recurrent redox oscillations in permeable sediments [17]. In the mangrove sediment, sulphide, H_2 and organic C compounds are common electron donors [18, 19] and oxygen, sulphate, nitrate and Fe(III) are major electron acceptors, which co-exist along the sediment depth [20]. The vertical distribution of electron donors and acceptors showed an obvious impact on microbial functions, such as anaerobic oxidation of methane (AOM) and sulphate reduction [21, 22]. Recently, we found that N_2 fixation rate increased while the diversity of diazotrophic communities decreased along the depth of mangrove sediments largely due to the vertical variation of salinity [23]. However, most of such studies were focused exclusively on the top 20 cm of mangrove sediments, which was considered as the layer with the greatest microbial diversity, biomass and activity [6, 20, 24]. Therefore, a comprehensive profile of CH_4, N and S cycling genes/pathways along a vertical gradient of mangrove sediments is crucial for predicting mangrove ecosystem functions.

Generally, microbes in natural ecosystems do not exist independently, and they interact with each other to form complex microbial communities and couple with different biogeochemical cycling processes. Microbial interactions have been well investigated in the laboratory [25] or in several natural ecosystems such as lakes [26, 27] and marine sediments [28, 29]. For example, nitrate reduction could be coupled with S oxidation by a single organism [30] or syntrophic microbial consortia [28]; anaerobic CH_4 oxidizers (ANMEs) and sulphate-reducing bacteria (SRB) or S-disproportionating bacteria were found to be syntrophic partners responsible for anaerobic CH_4 oxidation and sulphate reduction in anoxic CH_4-rich sediments [29, 31]. However, such microbial interactions in mangrove sediments remain poorly understood due to their extremely high diversity and the as-yet uncultivated status of major environmental microorganisms. Metagenomic analysis provides the possibility to explore the potential microbial interactions without the limitation in terms of uncultivated microbes [26, 32]. Thus, it could be important to understand the microbially driven CH_4, N and S cycling as well as their coupling mechanisms by metagenome sequencing analysis, which may enable us to develop novel strategies for enhancing mangrove ecosystem functions and mitigating climate change.

In this study, we aimed to understand the vertical distribution of microbially driven CH_4, N and S cycling and their potential coupling mechanisms in mangrove ecosystems. Due to the vertical changes of nutrients (e.g. total C, total N), electron status (e.g. acid volatile sulphide, SO_4^{2-}), and/or environmental conditions (e.g. pH, temperature) [6, 33], we hypothesized that the overall functional diversity of sedimentary microbial communities would decrease, their functional composition and interactions would shift as the depth increased, and S cycling microbes could play an important role in coupling biogeochemical cycling processes due to their metabolic versatility in response to mangrove sedimentary nutrients, electron acceptors and donors, and environmental conditions at different depths [34, 35]. To test the hypotheses, we collected 0–100-cm sediment samples from the Qi'ao Mangrove Reserve in Zhuhai, China. The vertical profile of CH_4, N and S cycling genes/pathways was analysed by metagenome sequencing approaches, and their possible coupling mechanisms among CH_4, N and S cycling were explored. This study provides a comprehensive perspective of vertical distribution of CH_4, N and S metabolisms at a fine spatial scale and improves our

understanding of their possible coupling mechanisms in mangrove sediments.

Methods

Sample collection and processing

The sampling site is located at the Qi'ao Mangrove Reserve (22.42° N, 113.63° E) in Zhuhai, China. Five 1-m plunger cores were collected as replicates from a mangrove habitat dominated by *Kandelia obovata* in December 2019 (Additional file 1: Fig. S1). The sediment cores were divided into 10 depths (i.e. 0–5, 5–10, 10–15, 15–20, 20–30, 30–40, 40–50, 50–60, 60–80 and 80–100 cm), resulting in a total of 50 samples. These samples were stored in a portable cooler at 4°C and transported to the laboratory within 24 h. Each sample was divided into two subsamples: one was immediately stored at −80°C for DNA extraction, and the other was stored at 4°C for physicochemical analysis.

Sediment physicochemical properties analysis

Temperature and pH of sediment were measured in situ by a hand-held metre (Extech Instruments, A FLIR Company, USA). Salinity was determined with 2.0 g dry sediment in a 1:5 sediment/water suspension with a salinity metre (EUTECH SALT6þ, Thermo Scientific, USA). Soil ammonium (NH_4^+), nitrite (NO_2^-) and nitrate (NO_3^-) were extracted using 2 M KCl and measured with a multimode microplate reader (Varioskan LUX, Thermo Scientific, USA). Porewater sulphate (SO_4^{2-}) concentration was measured with porewater extracted from 10.0 g fresh sediment by an ion chromatography (Dionex ICS-1100, Thermo Scientific, USA). Acid volatile sulphide (AVS) was treated with acid to release H_2S and measured by iodometric titration method [36]. S^0 was measured with a high-performance liquid chromatograph (Agilent 1260 Infinity II, Agilent, Germany). Sediment samples for measuring the total carbon (TC), total nitrogen (TN) and total sulphur (TS) were dried at 65°C until reaching a constant weight, finely ground, and then measured by an elemental analyser (Vario TOC, Elemental, Germany).

Sediment DNA extraction and shotgun metagenome sequencing

Sediment microbial community DNA was extracted with 5.0 g fresh sediment using a modified freeze-grinding plus sodium dodecyl sulphate (SDS) lysis method as described previously [37], and purified by Power Soil DNA Isolation Kit (Mo Bio Laboratories, Carlsbad, California, USA). DNA quality was assessed by a Nanodrop (NanoDrop One, Thermo Scientific, USA), all the DNA kept in subsequent experiment with the ratios of 260/280 nm and 260/230 nm were around 1.8 and above 1.7, respectively. The final DNA concentration was quantified by a fluorescent method (Qubit 4 Fluorometer, Thermo Scientific, USA).

All 50 samples were subjected to shotgun metagenome sequencing. Dual-indexed DNA sequencing libraries were constructed using NEBNext® UltraTM DNA Library Prep Kit for Illumina (NEB, USA) according to the manufacturer's recommendations. Prepared library DNA concentrations were determined with a Qubit HS DNA assay and libraries were run on a High Sensitivity DNA chip using the Agilent 2100 Bioanalyzer to determine library average insert sizes. After cluster generation was performed on a cBot Cluster Generation System, paired-end reads (PE150) were sequenced in Guangdong Magigene Biotechnology Co., Ltd. with an Illumina HiSeq2500 platform. For each sample, approximately 10 Gb of metagenome sequencing data (33,504,696 to 67,951,834 reads per sample) (Additional file 1: Table S1) was generated after adapter trimming and sequence filtering. Specifically, the paired reads with more than 10% unknown bases ('N' bases) or more than 50% of low-quality bases (quality value ≤ 5) in any read were removed [38].

Read-based functional and taxonomical analysis

The raw data were further quality-trimmed with BBDuk (k=28 mink=12 trimq=20 minlength=70) (https://jgi.doe.gov/data-and-tools/bbtools/bb-tools-user-guide/bbduk-guide/), and the sequence quality was assessed using FastQC (http://www.bioinformatics.babraham.ac.uk/projects/fastqc/). Qualified metagenomic paired-end reads were merged using PEAR (options: -p 0.001) [39], and the merged sequences were used for functional annotation and taxonomic assignments.

Gene prediction was carried out by Prodigal (https://github.com/hyattpd/Prodigal), which could predict high-quality gene fragments from merged short reads. The predicted gene fragments were searched against KEGG (http://www.genome.jp/kegg/pathway), MCycDB [40], SCycDB [41] and NCycDB [42] reference databases using DIAMOND [43] (options: -k 1 -e 1E-5-sensitive) for functional annotation. All samples were rarefied to the same sequencing depth (6,779,669 sequences per samples) by random resampling. The relative abundance of genes was defined as the number of gene sequence reads. The obtained functional profiles of KO terms, CH_4, N or S cycling gene families were used for the subsequent analysis.

The overall taxonomic assignments of microbial communities were assessed using the phylogenetic annotation of merged reads with Kraken2 [44]. The genetic potential of a specific pathway was analysed following the key gene families involved in CH_4, N and S cycling. The reads related to each key gene family were retrieved using SeqKit [45]. The taxonomic placement of each read was

inferred for searching the Kraken2 database. The representatives of key gene families were further analysed, including *mcrA* for methanogenesis and *pmoA* for aerobic oxidation of CH_4; *nrfA* for dissimilatory nitrate reduction (DNRA), *nifH* for N fixation, *narG*, *nirS*, *nirK*, *norB* and *nosZ* for denitrification, and *hzsA* for anammox; *soxB*, *sqr* and *fccB* for S oxidation, *asrB* for S reduction and *sat*, *aprA*, *dsrA* and *dsrB* for dissimilatory sulphate reduction or S oxidation.

Metagenome sequence assembly, binning and genome annotations

Quality-filtered reads were assembled to contigs with MEGAHIT [46] at the default mode according to the MetaWRAP analysis workflow. Open reading frame (ORF) fragments were predicted using Prodigal and searched against MCycDB [40], SCycDB [41] and NCycDB [42]. All target sequences were retrieved and taxonomically annotated using Kraken2. Their abundances were estimated using Salmon [47] and normalized into Transcripts Per Million (TPM) counts. Binning was conducted using MetaBAT2 (v2.12.1) [48] and the resulting bins were consolidated with the Bin_refinement module. The bins were dereplicated with dRep [49] with a secondary cluster ANI 99% (strain level). CheckM [50] was used to assessed the quality score (completeness – 5*contamination) of genome bins and only genomes with a quality score of ≥60 were retained [51, 52]. This resulted in a total of 77 high-quality dereplicated genome bins, hereafter referred to as metagenome-assembled genomes (MAGs). The relative abundances of MAGs in different samples were assessed with CoverM (https://github.com/wwood/CoverM). The taxonomy of MAGs was assigned with GTDB-Tk v1.3.0 reference data version r95 [53], and their gene predictions were performed using Prodigal, and the predicted genes were further annotated using METABOLIC [54] and eggNOG-mapper [55].

Molecular ecological network construction and analysis

To explore how microbes and key genes involved in CH_4, N and S cycling processes interact in the mangrove sediment, we constructed molecular ecological co-occurrence networks based on the microbes involved in CH_4, N and S cycling. We grouped all 10 depths into three layers: surface (0–15 cm), middle (15–30 cm) and deep (30–100 cm) layers based on multiple response permutation procedure (MRPP), and analysis of similarity (ANOSIM) among functional profiles of microbial communities from different depths (Additional file 1: Table S2, Table S3). Three co-occurrence networks were constructed based on taxonomic profiles, which were generated from the taxonomy of all contigs involved in CH_4/N/S cycling processes. The networks were constructed using the Molecular Ecological Network Analyses (MENA) pipeline [56], which implements Random Matrix Theory (RMT) to identify thresholds for constructing highly confident microbial ecological networks. Only taxa representing in half or more samples were selected to calculate the Spearman correlation coefficient (r), and the minimum threshold of $r = 0.8$ was automatically determined by the RMT approach. Network topological parameters were calculated by the MENA pipeline. The within-module connectivity (Z_i) and among-module connectivity (P_i) of each node were calculated to define their roles in the networks: peripherals ($Z_i < 2.5$, $P_i < 0.62$), connectors ($Z_i < 2.5$, $P_i > 0.62$), module hubs ($Z_i > 2.5$, $P_i < 0.62$) and network hubs ($Z_i > 2.5$, $P_i > 0.62$). The latter three were regarded as keystone taxa because of their important roles in network topology. The constructed microbial networks were visualized by Cytoscape [57].

Statistical analysis

Following analyses were performed to test whether gene families display associations with environmental variables. First, Mantel tests were used to determine the linkage between environmental variables and CH_4/N/S cycling gene abundances. Second, the maximal information coefficient (MIC) was estimated to capture diverse relationships between gene families and environmental factors [58], and relationships with MIC ≥0.4 were considered statistically significant. The MIC value significance was assessed using precomputed P values. And we used the percentage of genes that were significantly (MIC score ≥0.4) associated to an environmental variable among the total of genes involved in a pathway to estimate the importance of an environmental variable to a specific pathway. The α-diversity (Shannon index) of sediment microbial communities was calculated based on resampled functional and taxonomical profiles using the Galaxy pipeline (http://192.168.3.11:8080/), and their β-diversity was estimated using principal coordinates analysis (PCoA) based on the Bray–Curtis distance. ANOSIM and MRPP were used to evaluate the significance of compositional differences between functional diversity and sediment depths. Linear regression was used to explore the relationship between the abundance of key genes and sediment depths. One-way analysis of variance (ANOVA) was performed with the IBM SPSS 22 (SPSS Inc., USA) to compare the mean of sediment parameters, functional diversity and abundances among different depths. Spearman analysis was performed to estimate the correlation between key genes. All the statistical analyses were visualized using R packages including Minerva [59], reshape2 [60], rstatix [61], vegan [62], ggplot2 [63] and pheatmap [64] and GraphPad Prism 8.0.

Results

Vertical variation of physicochemical properties in mangrove sediments

We measured sediment pH, temperature, salinity, SO_4^{2-}, AVS, S^0, NH_4^+, NO_2^-, NO_3^-, TC, TN and TS to characterize the vertical distribution of environmental factors in mangrove sediments (Additional file 1: Table S4). The results showed that pH and temperature significantly ($P < 0.05$; multiple comparison with one-way ANOVA analysis) increased with the depth, while salinity, TC, TN, SO_4^{2-} and AVS showed an opposite trend. The sediment had higher concentrations of NH_4^+ (1800–4700 μg/L) relative to NO_3^- (88.3–294.9 μg/L) or NO_2^- (58.9–103.9 μg/L), and the maximum NH_4^+ concentration appeared at the 5–10 cm sediment depth. Additionally, the concentrations of S^0 and TS did not change through the vertical profile.

Environmental drivers of CH_4, N and S cycling microbiomes

To disentangle potential environmental drivers of microbiome functions in mangrove sediments, we performed Mantel tests and estimated the maximal information coefficient (MIC) value between physicochemical properties and the abundance of gene families involved in CH_4/N/S cycling. The results showed that pH and AVS were the dominant factors shaping the functional diversity and composition of CH_4, N and S cycling microbiomes, and followed by SO_4^{2-} and NO_3^- along the sediment depth (Fig. 1A, B). Specifically, pH showed significantly ($P < 0.001$) positive correlations with the relative abundance of functional genes involved in CH_4, N and S cycling (Additional file 1: Table S5), and had a high importance in structuring these metabolic pathways in mangrove sediments, explaining 81.3% of the turnover of denitrification gene families, 76.5% for dissimilatory nitrate reduction (DNRA), 57.7% for S reduction, 69.2% for methanogenesis and 61.5% for aerobic oxidation of CH_4 (Fig. 1C). Additionally, AVS was found to have the largest influences on denitrification and S oxidation, explaining 87.5 and 95.0%, respectively, while nitrate showed the greatest effect on Sox systems and S oxidation, explaining 85.7 and 90.0%, respectively. Collectively, the results revealed the importance of pH and AVS for driving the depth-dependent variability of microbially mediated CH_4, N and S cycling processes, where AVS could be an important electron donor for nitrate reduction in mangrove sediments.

An overview of metagenomic characteristics of mangrove sediment microbiomes along the sediment depth

To survey metagenomic characteristics along the sediment depth, we analysed the functional and taxonomical profiles based on metagenome sequencing data. We found distinct variation trends of functional and taxonomical diversity along the depth. Specifically, the overall functional α-diversity (based on KO terms) of microbial communities decreased with increasing depths (Fig. 2A). The functional diversity of N and S cycling communities deceased as sediment depths increased, while that of CH_4 cycling communities did not show significant differences among depths (Fig. 2A). However, the overall taxonomical α-diversity of microbial communities as well as CH_4, N and S cycling communities all increased with the sediment depth (Fig. 2B). Most of bacterial metagenome reads were matched to *Proteobacteria* (58.0–68.0%), and their relative abundances decreased significantly ($R^2 = 0.63$, $P < 0.001$) along the sediment depth. Archaeal metagenome reads were mostly assigned to *Euryarchaeota* (0.8–2.3%), which showed a significantly (R^2=0.19, $P < 0.05$) increasing trend along the sediment depth (Additional file 1: Fig. S2). Additionally, both functional and taxonomical profile-based principal coordinates analysis (PCoA) revealed that the sediment microbial community composition and structure significantly ($P < 0.001$, ANOSIM) shifted with the sediment depth (Additional file 1: Fig. S3, Fig. S4), suggesting that CH_4, N and S cycling microbiomes were sensitive to the sediment depth.

Vertical profiles of CH_4/N/S cycling genes/pathways and taxa

To further understand the vertical distribution of functional genes and pathways of CH_4, N and S cycling microbiomes, we analysed the functional composition of microbial communities with a focus on the relative abundance of key functional genes and pathways involved in CH_4, N and S cycling (Fig. 2C), and a notable divergence of these metabolic patterns among different sediment depths was observed.

(i) *CH_4cycling*. We estimated the relative abundance of functional genes related to methanogenesis and methane oxidation. Our data showed a high percentage of metagenome reads matched central methanogenic pathways (21.8–28.6%) (Additional file 1: Fig. S5). The relative abundance of methyl coenzyme M reductase gene (*mcrA*) increased along the depth, whereas low frequencies of *pmoA* gene families were detected with a reverse trend (Fig. 2C, Additional file 1: Fig. S6). The main taxa responsible for methanogenesis were found to be *Methanolinea* (hydrogenotrophic methanogens), *Methanoregula* (hydrogenotrophic methanogens) and *Methanothrix* (acetoclastic methanogens). CH_4 oxidizing bacteria were rarely obtained, appearing to be predominated by *Methylomicrobium*, *Methylomonas* and *Methylocystis* (Fig. 3). These results

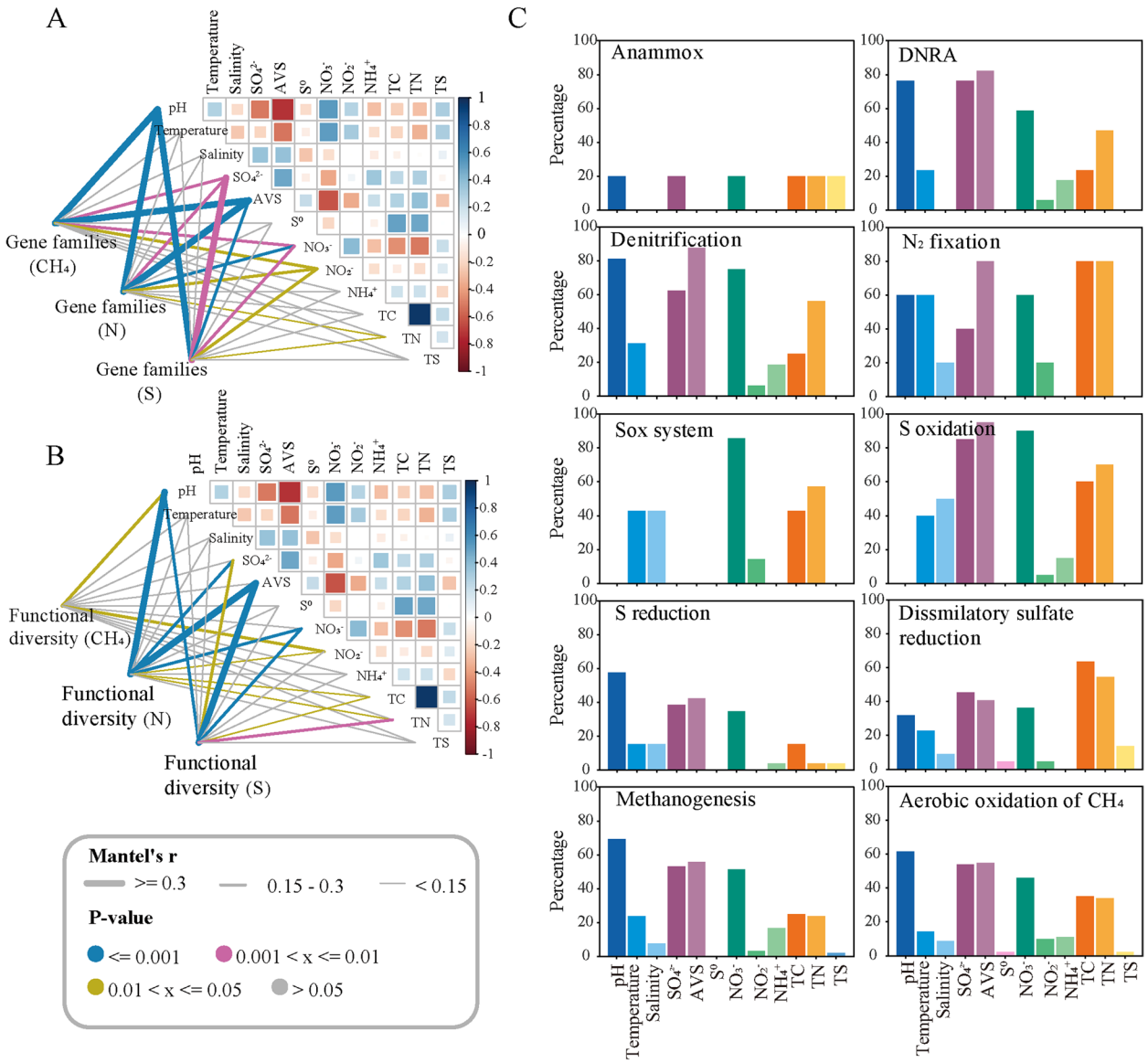

Fig. 1 Associations between environmental factors and functions of mangrove sediment microbiomes. Mantel tests revealed the correlation between environmental factors and CH_4/N/S cycling gene families (**A**), or functional diversity (**B**). **C** The importance of individual environmental factors to a specific metabolic pathway involved in CH_4/N/S cycling was calculated using the maximal information coefficient (MIC) index. The percentage refers to the percentage of gene families involved in the specific metabolic pathway significantly driven by environmental factors. DNRA: dissimilatory nitrate reduction

indicated relatively high abundances of gene families involved in methanogenesis were distributed in deep sediments, and methane production was mainly performed by hydrogenotrophic and aceto-clastic methanogens.

(ii) *N cycling*. The metagenome reads mapped to the N cycle were mainly related to nitrate reduction with 15.4–16.5% for DNRA, 11.6–14.0% for denitrification, and 64.6–68.0% for organic N degradation and synthesis (Additional file 1: Fig. S5). First, gene families (*ureABC* and *gdh*) involved in organic N decomposition significantly ($P < 0.05$) decreased along the depth, which may explain high concentrations of NH_4^+ in the surface sediment to some extent. Second, all gene families involved in denitrification (*narG*, *nirK*, *nirS*, *norB*) were detected with high relative abundances but with a decreased trend along the sediment depth except *nosZ* (Fig. 2C, Additional file 1: Fig. S7), and the major denitrifying taxa included *Pseudomonas*, *Cupri-*

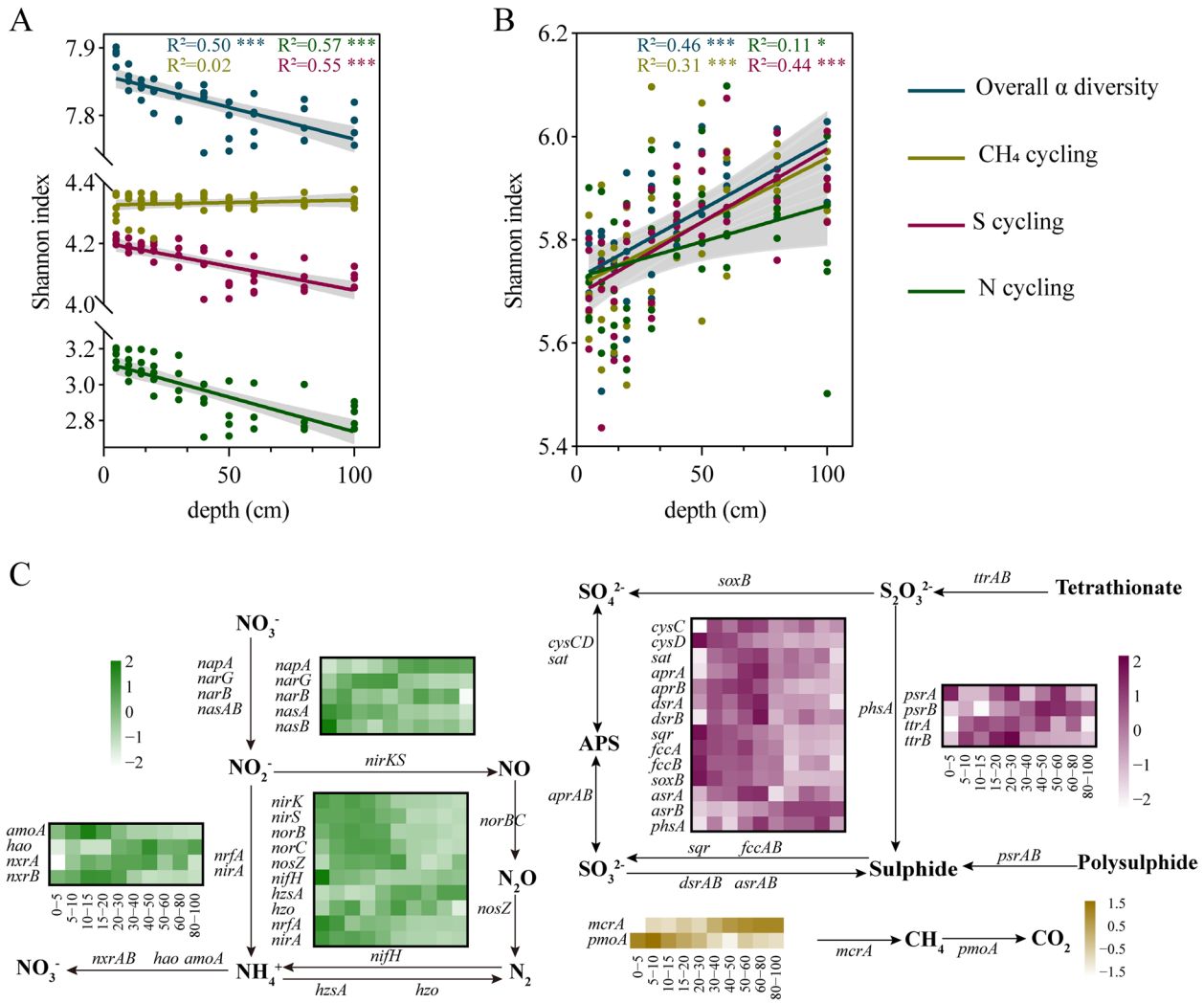

Fig. 2 Depth variations of functional potentials of mangrove sediment microbiomes. **A** Relationships between functional diversity and sediment depths. **B** Relationships between taxonomical diversity and sediment depths. **C** Heatmaps of *Z*-score normalized relative abundances of key genes involved in CH_4/N/S cycling. Blue dots/lines indicate the overall functional/taxonomical diversity of microbial communities; yellow dots/lines indicate the functional/taxonomical diversity of methane cycling communities; green dots/lines indicate the functional/taxonomical diversity of nitrogen cycling communities; purple dots/lines indicate the functional/taxonomical diversity of sulphur cycling communities. Grey shaded areas represent 95% confidence intervals. R^2 was obtained by linear regression analysis and *P* was obtained by Pearson's correlation analysis. *($0.01 < P < 0.05$), **($0.001 < P < 0.01$) and ***($P < 0.001$)

avidus, *Azoarcus*, *Sulfurifustis* and *Thauera* (Fig. 3, Additional file 1: Fig. S8). Third, the detected *nrfA* gene (the marker gene of DNRA) was largely affiliated with *Anaeromyxobacter*, *Geobacter* and *Desulfovibrio*, and their relative abundances decreased along the depth, whereas *nifH* gene originated from *Desulfovibrio*, *Geobacter* and *Bradyrhizobium* did not show differences among different sediment depths (Figs. 2C and 3, Additional file 1: Fig. S7). Fourth, the relative abundances of anammox genes (e.g. *hzo*, *hzsA*) were low, and a small number of metagenome reads were assigned to ammonia oxidizers. The results indicated that ammonification and nitrate reduction showed high functional potentials in the surface sediment (0–15 cm), and taxonomic groups responsible for nitrate reduction (denitrification and DNRA) were related to S-oxidizing bacteria and SO_4^{2-}-reducing bacteria.

(iii) *S cycling*. For the S cycle, the metagenome reads were largely mapped to organic S transformation (38.8–42.7%) and transformation between inorganic S and organic S (15.9–21.4%) (Additional file 1: Fig. S5). S oxidation genes (e.g. *fccAB* and *sqr* for sulphide oxidation, *soxB* for thiosulphate oxida-

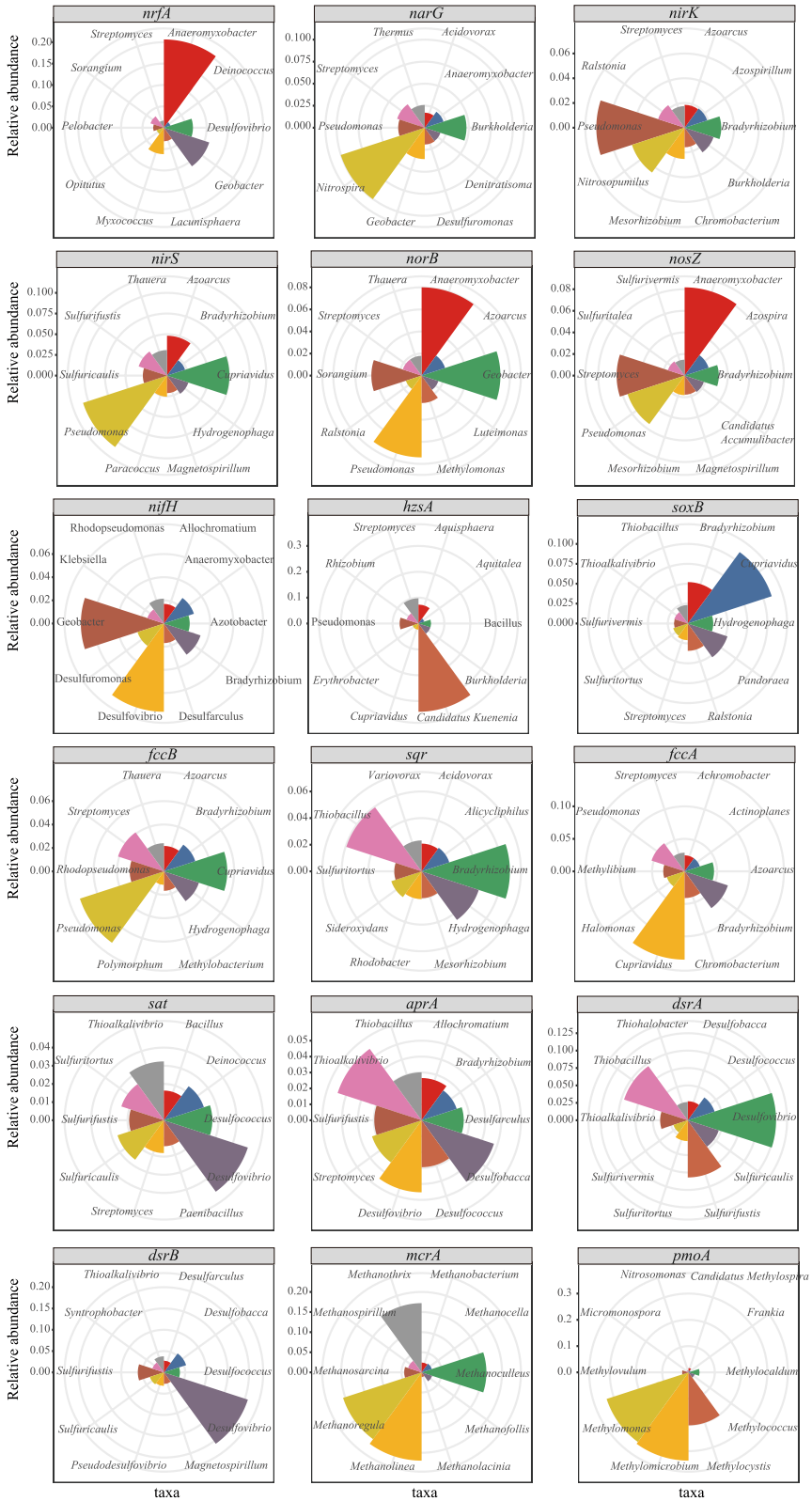

Fig. 3 A summary of key microbial taxa involved in CH_4, N and S cycling. The percentage of relative abundances for the top 10 abundant microbes involved in each key gene family is shown in the wind rose diagrams

tion to sulphate) significantly ($P < 0.05$) decreased as depth increased, suggesting active S oxidation potentials in the surface sediment (Fig. 2C, Additional file 1: Fig. S9). These key S oxidation genes (*soxB*, *fccB* and *sqr*) were mostly affiliated with *Cupriavidus*, *Bradyrhizobium* and *Hydrogenophaga* (Fig. 3, Additional file 1: Fig. S8), pointing to the important role of these genera in S oxidation in mangrove sediments. Also, the relative abundance of gene families responsible for polysulphide reduction (*psrB*) and sulphite reduction (*asrB*) significantly ($P < 0.05$) increased along the depth (Fig. 2C, Additional file 1: Fig. S9), which were mostly affiliated with *Geobacter*, *Pseudomonas*, *Streptomyces* and *Desulfovibrio*. Additionally, the relative abundance of *sat* and *aprAB* for dissimilatory sulphate reduction increased at the depth of 0–30 cm and then decreased, while *dsrAB* exhibited no differences along the depth, which were affiliated with S-oxidizing bacteria (SOB) (dominated by *Thioalkalivibrio*, *Sulfurifustis*, *Sulfuricaulis* and *Thiobacillus*) and sulphate-reducing bacteria (SRB) (dominated by *Desulfovibrio*, *Desulfobacca* and *Desulfococcus*) (Figs. 2C and 3, Additional file 1: Fig. S9). The results indicated that S oxidation had high functional potentials in the surface sediment (0–15 cm), and sulphate reduction mainly occurred at the depth of around 30 cm. In view of taxonomical groups involved in denitrification and S oxidation, it is noted that S-driven denitrfiers, such as *Pseudomonas*, *Cupriavidus* and *Sulfurifustis*, could play an important role in coupling these two processes in the surface (0–15 cm) mangrove sediments.

Microbial co-occurrence networks in mangrove sediments

As key gene families involved in CH_4, N and S cycling showed distinct variation trends along the sediment depth, close correlations were detected among those processes. For example, gene families related to denitrification (*narG*, *nirK*, *nirS*, *norB* and *norC*) were significantly ($P < 0.05$) and positively correlated with S oxidation genes (*soxB*, *sqr* and *fccA*), suggesting a close relationship between these two processes (Additional file 1: Fig. S10). Also, significant ($P < 0.05$) and positive correlations were observed between *mcrABCD* gene families and *narG/nirK/nirS/norC/nosZ/asrB* gene families (Additional file 1: Fig. S10), indicating methanogenesis could be coupled with denitrification and sulphite reduction.

To further explore possible microbial interactions and coupling mechanisms at different depths, we constructed co-occurrence networks using taxonomical profiles associated with all contigs involved in CH_4, N and S cycling. Distinct structural and topological characteristics of CH_4, N and S cycling microbiome networks were observed (Fig. 4B). The mid-layer network appeared to possess the largest complexity with more nodes, more links, higher average clustering coefficient, higher node degrees and lower modularity compared with the surface and deep layer networks. There were 80.8% positive associations and 19.2% negative associations in the mid-layer, while 76.0% positive and 24.0% negative associations in the surface layer, and 37.5% positive and 62.5% negative associations in the deep layer (Additional file 1: Fig. S11).

We also identified potential keystone species, including module hubs, network hubs and connectors based on within-module connectivity and among-module connectivity values. Only one module hub (*Sulfuricaulis limicola*) was found in the surface layer network, but the mid-layer network had eight module hubs: *Betaproteobacteria taxid* (28216), *Desulfomicrobium orale* DSM, *Desulfovibrio desulfuricans*, *Methanoregula boonei*, *Methylobacterium* sp. 17SD2-17, *Proteobacteria taxid* (1224), *Rhizobiales taxid* (356) and *Thioalkalivibrio sulfidiphilus* HL-EbGr7 (Fig. 4A). These potential keystone species were positively interacted with other microbial groups and could form microbial syntrophies in the middle mangrove sediments. Also, sulphate-reducing bacterium *Desulfovibrio desulfuricans* appeared to positively interact with methanogens (*Methanoculleus*, *Methanofollis* and *Methanolinea*), and *Methanoregula boonei* was positively correlated with *Desulfovibrio gigas* DSM in the middle layer, while those methanogens also had the maximal betweenness with other methanogens in the deep layer (Additional file 1: Table S6, Table S7), which mainly appeared to be hydrogenotrophic and acetoclastic methanogens. The results indicated that methanogens could potentially develop close relationships with SRB in the middle layer and with other methanogens in the deep layer.

Genomic capability of coupling CH_4, N and S cycling processes

Through metagenome assembly and binning, we further reconstructed 19 archaeal metagenome-assembled genomes (MAGs) and 58 bacterial MAGs (Additional file 2: Dataset S1). Among the archaeal MAGs, we retrieved five MAGs affiliated with *Methanoregulaceae*, *Methanoperedenaceae* and *Methanotrichaceae*, and they mainly distributed in deep sediment (Additional file 1: Fig. S12). *Methanoperedens* appeared to be an ANME with the marker gene (*mcrA*) for AOM, namely KO6. bin.60. Among the bacterial MAGs, we retrieved nine S-driven denitrifier MAGs containing key genes for S oxidation and denitrification, and nine MAGs for putative

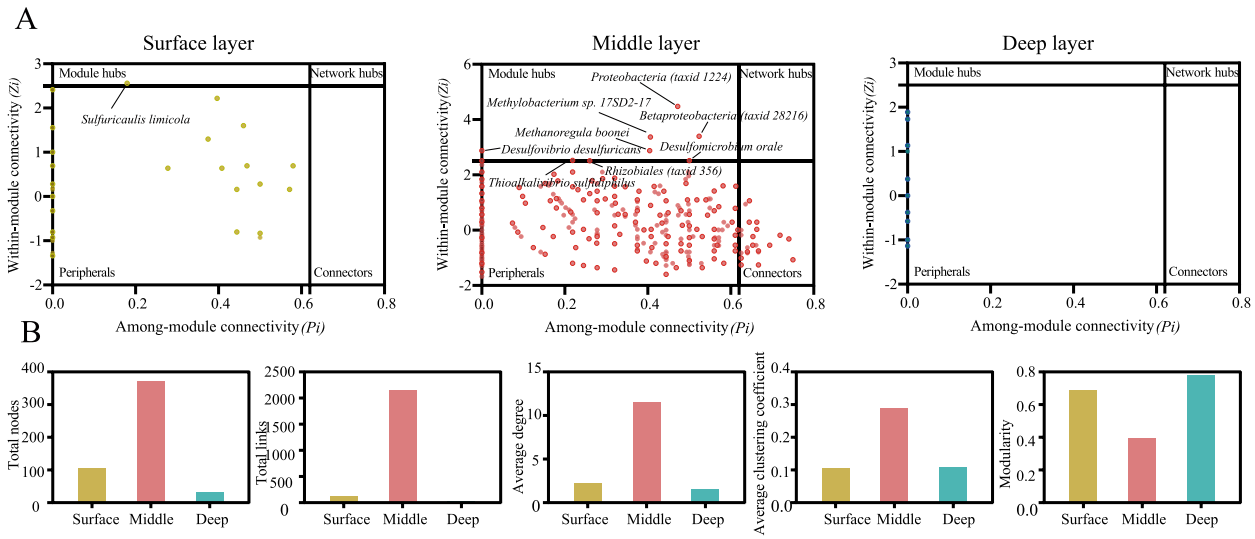

Fig. 4 The co-occurrence networks of microbial communities in the surface layer (yellow), middle layer (red) and deep layer (blue) sediments. **A** The network nodes were separated by within-module connectivity (Z_i) and among-module connectivity (P_i). Threshold values of Z_i and P_i for categorizing microbial taxa were 2.5 and 0.62, respectively. **B** The overall topological characteristics at different sediment layers

SRB with *dsrABD* genes or affiliated with *Desulfobacterota*. Only one MAG (KO6.bin.24) from the phylum *Desulfobacterota* encoded *dsrD* (Additional file 1: Fig. S13A, Fig. S14, Additional file 2: Dataset S2).

S-driven denitrifier MAGs were distributed throughout *Thermodesulfovibrionia* (KO2.bin.92, KO2.bin.52), *Desulfobacterota* (KO5.bin.170, KO6.bin.144), *Sulfurifustis* (KO5.bin.162), *Chloroflexota* (KO5.bin.187), *Alphaproteobacteria* (KO6.bin.124) and *Burkholderiales* (KO6.bin.19, KO8.bin.148) (Fig. 5). The relative abundances of these MAGs were higher in the surface and middle sediments than those in the deep sediment (Additional file 1: Fig. S13B). All S-driven denitrifier MAGs could use different N species as electron acceptors except N_2O, which could lead to N_2O production in the sediment. Among them, six MAGs harboured sulphide:quinone oxidoreductase (Sqr), which catalyses the oxidation of sulphide to elemental sulphur (Fig. 5).

As a representative genome for SRB, *Desulfurivibrionaceae* (KO6.bin.24) contained core enzymes involved in SO_4^{2-} reduction, including adenylylsulphate reductase alpha subunits (AprA), and dissimilatory sulfitereductase alpha, beta and delta subunits (DsrABD) except sulphate adenylyltransferase (Sat). It also contained electron transport complexes QmoAB and DsrMKJOP, and the sulphur relay protein DsrC. Additionally, a sulphur transporter (ThiF) was also detected in this *Desulfurivibrionaceae* genome (Fig. 6, Additional file 2: Dataset S3).

As a representative ANME, *Methanoperedens* (KO6.bin.60) contained core enzymes involved in AOM except methenyl-H_4MPT cyclohydrolase (Mch) and formyl-MFR:H_4MPT formyltransferase (Ftr): formyl-MFR dehydrogenase (Fmd), methylene-H_4MPT dehydrogenase (Mtd), methylene-H_4MPT reductase (Mer), methyl-H_4MPT:HS-CoM methyltransferase (Mtr) and methyl-CoM reductase (Mcr). It also contained the heterodisulfide reductase (Hdr), F_{420} hydrogenases (Fpo) and some extracellular electron transfer proteins, such as archaeal type IV pilus (PilTC) and archaeal flagellin (FlaD). Additionally, sulphur-related enzymes were detected in this genome, such as sulphur transfer proteins (TauE) and sulphide dehydrogenase (SudB), which could reduce S^0 to sulphide (Fig. 6, Additional file 2: Dataset S4).

Discussion

Revealing the vertical profile of CH_4, N and S cycling genes/pathways and associated taxonomic groups as well as their potential coupling mechanisms is crucial to understand mangrove ecosystem functioning. In this study, we analysed the metabolic landscape of CH_4, N and S cycling microbial communities to decipher potential interactions among functional members. Our results clearly demonstrated a decreased trend of the overall functional diversity of microbial communities along the sediment depth, and a strong vertical stratification of microbial functional genes/pathways was predominantly driven by AVS and pH, especially high abundances of key gene families involved in denitrification and S oxidation distributing in the surface layer and relatively high abundances of key gene families involved in methanogenesis distributing in the deep layer. Complex microbial interactions were found in the surface and middle layers with S

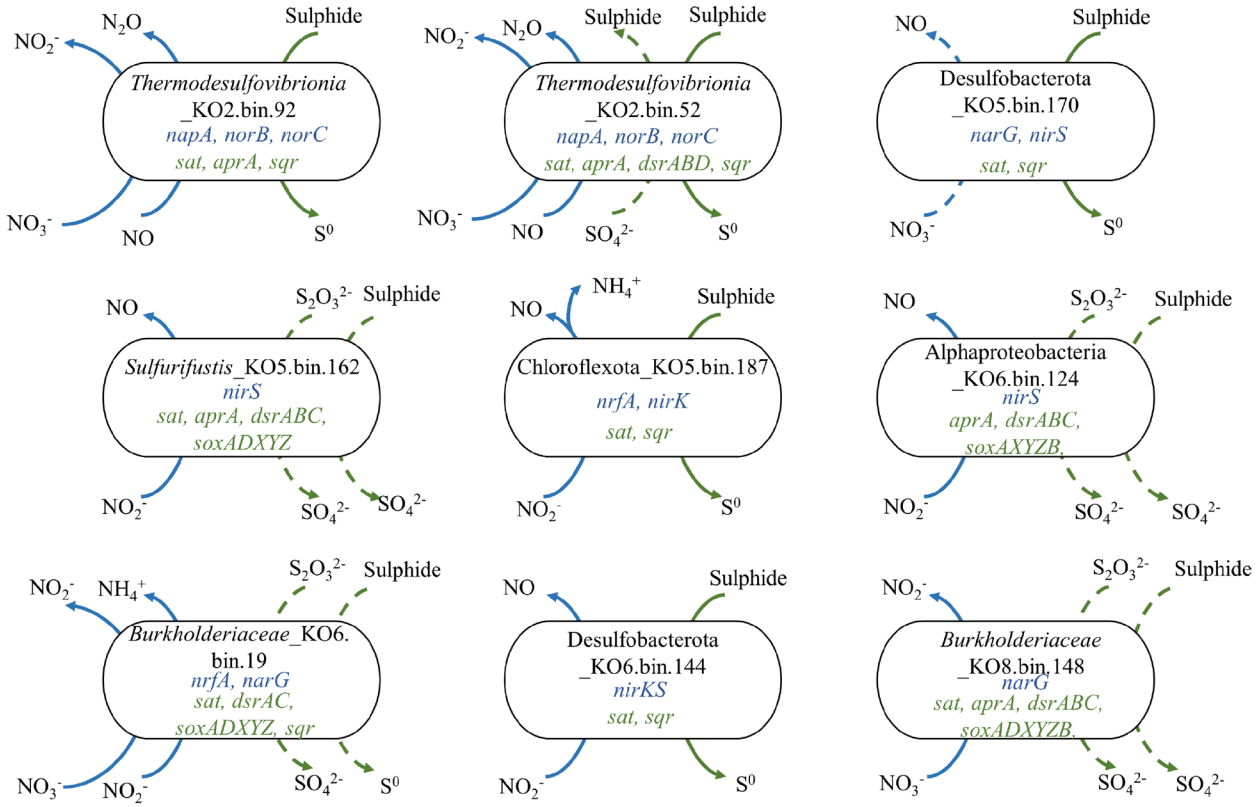

Fig. 5 Metabolic characteristics of nine S-driven denitrifiers on denitrification and S oxidation in mangrove sediments. Blue arrows indicate denitrification reactions and green arrows indicate S oxidation reactions. Solid arrows represent the reactions found in the recovered MAGs and dashed arrows indicate omitted reactions. A detailed list of genes in these S-driven denitrifiers can be found in Additional file 2: Dataset S3

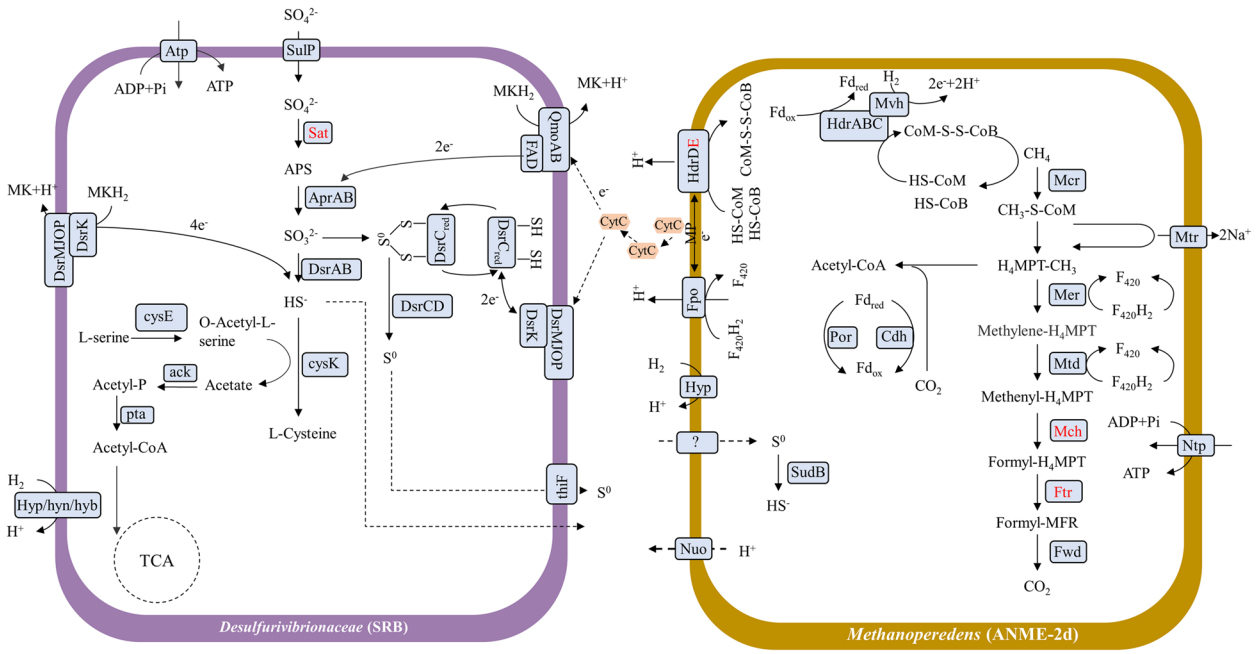

Fig. 6 Possible coupling pathways of anaerobic oxidation of methane and sulphate reduction inferred from the MAGs of *Methanoperedenaceae* and *Desulfurivibrionaceae*. Absent enzymes were in red colour; dashed arrows indicate unknown pathways. The detailed list of genes in these genomes can be found in Additional file 2: Dataset S3 and Dataset S4

oxidation coupled with denitrification in the surface sediment, and SRB with methanogens/ANMEs in the middle layer. These results generally support our core hypothesis that fluctuating environmental conditions would lead to a notable divergence of metabolic patterns of CH_4/N/S cycling, and S cycling microbes could play important roles in coupling CH_4 and N cycling processes in mangrove sediments.

CH_4 cycling is an important process of the C cycle, and its emissions significantly offset the C burial in mangrove sediments, accelerating global warming [65]. Previous studies showed that the abundance of methanogenesis genes increased with the mudflat sediment depth [66], and the composition of methanogens showed obvious variations in different ecosystems [6, 67]. For example, hydrogenotrophic methanogenesis was dominated in a subseafloor sediment [68], peatlands [69] and mangrove sediments [70]. In this study, we observed a relatively high abundance of *mcrA* gene and an increasing trend along the sediment depth, suggesting a possibly more active methanogenesis in the deep sediment. Also, *Methanolinea* and *Methanoregula* of the order *Methanomicrobiales* were found to be the dominant methanogenic genera. This finding is consistent with previous studies in the Sanjiang Mire Wetland, Ruoergai peatland, Hongze wetland and Poyang wetland [71], indicating that hydrogenotrophic methanogenesis may dominate CH_4 production in mangrove sediments. Specifically, *Methanoregula boonei* as a H_2-utilizing methanogen was identified as a keystone in the middle mangrove sediment, and it also had the maximum betweenness with other methanogens in the deep sediment. As *M. boonei* generated ATP using protons with membrane-bound methyltransferase rather than sodium ions, hydrogen might be transferred from other methanogens to *M. boonei* to conserve energy with close interactions between them [72, 73]. Therefore, the close interactions among methanogens in deep sediments might contribute to the CH_4 generation and regulating CH_4 emissions in mangrove sediments [74]. In addition, low abundances of *pmoA* gene were detected and their abundances decreased with the sediment depth, which was consistent with previous studies [75, 76].

Microbially driven N cycling is critical to maintain N nutrients for mangrove growth in such N-limited ecosystems. Denitrification is considered as the major N-loss pathway in mangrove sediments through the production of N_2O (a strong greenhouse gas) and/or N_2 [9], while another N-loss pathway, anammox, was found to mainly occur in shallow wetland soils associated with high concentrations of NH_4^+ as substrate in previous studies [14, 77]. In contrast to anammox and denitrification, dissimilatory nitrate reduction to ammonium (DNRA) reduces nitrate to NH_4^+ and was found to alleviate N limitation of mangrove ecosystems [78]. Our results showed higher functional potentials of denitrification in the surface sediment compared to the deep sediment, consistently with previous studies [16], which could be explained by two possible mechanisms: (i) co-respiration of NO_x^- and O_2 [17] and (ii) closely coupled nitrification–denitrification in microenvironments [79]. Therefore, our results implied that some denitrifying bacteria could adapt to tidally induced recurrent redox oscillations and/or tolerate certain concentrations of O_2 and perform denitrification in the surface sediment. Differently from previous studies, we found an increasing trend of anammox along the sediment depth, mainly due to competition for inorganic N compounds by growing plants [80] or heterotrophic nitrate- and nitrite-reducing bacteria. In addition, due to the reduction of root density along mangrove sediments [81], the N demand for mangrove growth decreased. High NH_4^+ concentration, organic N decomposition and DNRA potential were observed in the surface sediment, suggesting high demands of N supply in the surface sediment, and these two processes may contribute to an important N sink in the surface mangrove sediment [82, 83].

For S metabolism, mangroves under macro-tidal regimes are rich in sulphate, driving efficient S cycling. Sulphate reduction is considered as the most important respiration process in mangrove sediments. The abundance of sulphate-reducing microorganisms is usually low in the uppermost oxygenated layers of sediments, while it reaches a maximum in the underlying anoxic zones and then decreases into the sulphate-depleted CH_4 zone [84, 85]. Due to the abundant sulphide produced by sulphate reduction in mangrove sediments, S oxidation may benefit plants by removing potentially toxic sulphide from the root zone [86]. Consistently with previous studies, a similar trend of gene families involved in sulphate reduction (*sat*, *aprA*, *aprB*) was observed in our study. However, the relative abundance of *dsrA* or *dsrB* did not show significant differences along the sediment depth, probably because both genes are also involved in multistep processes of S oxidation as a reverse reaction for sulphate reduction [87]. Additionally, a high functional potential of S oxidation mainly performed by *Cupriavidus*, *Bradyrhizobium* and *Hydrogenophagain* was observed in the surface sediment in our study, where oxygen from recurrent tides and released by mangrove roots could provide suitable redox conditions for S oxidation [86]. Together, our study highlights that S oxidation and sulphate reduction may play an important ecological role in the surface and middle layer sediments, respectively, and high potentials of S metabolism may guarantee suitable conditions for mangrove growth.

Through developing diverse syntrophic partnerships, microorganisms could overcome thermodynamic barriers imposed by the environment to maintain their metabolic activities [88]. The co-occurrence networks constructed in this study showed potential microbial interactions of functional groups involved in CH_4, N and S cycling. Generally, a more complex network was found in the middle layer sediment as microbial interactions could be reduced due to heterogeneous environments in the surface sediment and excessive environmental pressures in the deep sediment [27]. Therefore, various syntrophic consortia could be responsible for diverse coupling mechanisms in different sediment depths.

It was proposed that denitrification coupled with S oxidation was crucial for the detoxification of sulphide in the mangrove sediment [19], which could be performed by a single autotrophic microbe such as *α-*, *β-*, *γ-* and *ε-proteobacteria* or by cooperation among those microorganisms [28, 89], indicating a diverse range of potential overlaps between denitrification and S oxidation. Previous studies showed that S-driven autotrophic denitrification coupling with the oxidation of reduced inorganic S compounds was widely distributed in the marine sediment [90] and soda lakes [91]. In this study, we identified a keystone SOB (*Sulfuricaulis limicola*) in the surface sediment, and observed strong correlations among gene families involved in S oxidation and denitrification as well except *nosZ* gene, suggesting a potential coupling mechanism of S oxidation with denitrification. As a N_2O sink, N_2O flux in mangrove sediments has ever been estimated ranging from −0.2 to 6.3 mg m^{-2} day^{-1} [92, 93], and denitrification could be responsible for up to 43 to 93% of N_2O production [94], indicating that denitrifiers play an important role in N_2O production. Diverse S-driven denitrifiers have been isolated from mangrove sediments, such as the centimetre-long bacterium *Candidatus (Ca.) Thiomargarita magnifica*, which could oxidize hydrogen sulphide and reduces nitrate, with ~75% of its total cell volume being occupied by a large nitrate-containing vacuole [95, 96]. Also, both read- and genome-level analyses found that *Cupriavidus* affiliated with family *Burkholderiaceae* and *Sulfurifustis* had the capability of S-oxidizing denitrification, which were found to be important contributors to both S oxidation and denitrification [97–99]. These findings suggest a more tremendous diversity of S-oxidizing denitrifier lineages in mangrove sediments than previously thought. Furthermore, previous studies found that high sulphide concentrations could inhibit nitrous oxide (N_2O) reductases [100, 101], and soil N–S interactions could substantially influence N_2O emissions [102]. In this study, all S-driven denitrifier MAGs lacked the *nosZ* gene, suggesting that such sulphide-utilizing groups might be an important contributor to N_2O production in the surface mangrove sediment [97]. Overall, the S-driven denitrifier-mediated N-S coupling reaction proceeds in the direction that is conductive to the sulphide detoxification, thus elucidating the metabolic mechanism of S-driven denitrification could regulate greenhouse gas emissions in the mangrove sediment.

The relationship of SRB and methanogens has been extensively studied in various environments such as marine sediments [103], salt marsh sediments [104] and mangrove sediments [105]. Although SRB were known to outcompete methanogens over common substrates, such as acetate and H_2, channeling the electron flow towards CO_2 production rather than methane [106], several studies showed that SRB and methanogens could co-exist under high sulphate concentrations, especially in the estuarine sediment [105, 107, 108]. In this study, we noticed that methanogens and SRB were keystones and positively correlated with each other, suggesting that they might co-exist in mangrove sediments. Although there are thermodynamic barriers of this interaction, we speculate that the co-occurrence between methanogens and SRB can be pulled forward upon the demand of ANME and SOB with recycling of metabolic products among them [109]. Enrichment experiments with deep groundwater indicated *Methanoperedenaceae* (ANME-2d) could conduct sulphate-dependent anaerobic oxidation of methane in the terrestrial subsurface [110]. Similarly, a *Methanoperedenaceae* MAG retrieved in this study had the metabolic potential for extracellular electron transfer to a syntrophic partner, such as flagella, which was previously reported to be an important feature of syntrophy establishments [111]. A previous study provided the genomic evidence that *Methanoperedenaceae* could acquire sulphur reduction genes by lateral gene transfer and might be involved in respiratory sulphur-dependent AOM [112]. The *Methanoperedenaceae* in this study also could encode sulphide dehydrogenase and reduce S^0, where the S^0 could form by SRB and be exported across the cytoplasmic membrane by ThiF protein, a sulphur exporter [113]. Also, methanotrophic archaea were found to produce S^0 during AOM and the produced S^0 would be disproportionated by the *Deltaproteobacteria* in a previous study [31], while our results suggest other possible mechanisms that *Methanoperedens* might directly transfer electrons to *Desulfurivibrionaceae*, or by AOM *Methanoperedens* could ultilize S^0 as an electron acceptor, which could be produced by *Desulfurivibrionaceae*. Recently, synthetic microbial ecology methods are considered as a novel approach to verify microbial interactions among different microorganisms like niche differentiation among different types of nitrifiers [114], but an experimental

verification of those potential syntrophic relationships is a great challenge due to the difficulty for isolating or culturing ANME or similar microorganisms.

As mangroves are located at the transition between ocean and land, the vertical variation of environmental factors caused by periodically tidal fluctuations play important roles in shaping the mangrove sediment microbiome structure [15]. Several previous studies showed that pH had a strong filtering impact on microbial communities [115, 116]. For instance, methanogens were sensitive to pH, which may affect acetate availability and directly impact acetoclastic methanogenesis, resulting in increased abundances of methanogens along the sediment depth [66, 117, 118]. Also, the availability of electron acceptors and donors could influence energetic metabolisms and further impact microbial functions [21, 22]. For example, the availability of electron acceptors (SO_4^{2-}, NO_3^-/NO_2^-, Mn_5^+) had a strong selective effect on ANMEs and then on CH_4 oxidation [119]. In this study, we found sediment niches of microbial communities differentiated from surface to deep layers, which was largely driven by various environmental factors including AVS and pH. First, AVS was detected as an important substrate for S oxidation and sulphate reduction in mangrove sediments, which could couple with nitrate reduction and methanogenesis, respectively, and the surface sediment with high concentrations of AVS showed high functional potentials of S oxidation, suggesting its important role in driving element cycles and sulphide detoxification for mangroves [10]. Second, increased pH could increase the relative abundance of *mcrA* gene in the deep sediment [120, 121], while neutral pH conditions might be suitable for methanogen growth [122]. Third, our study found that metabolic pathways of nitrate reduction were mainly driven by pH and AVS. This may be because that pH could directly affect the activity of enzymes involved in nitrate reduction and indirectly affect nitrate reduction by regulating the availability of organic C for

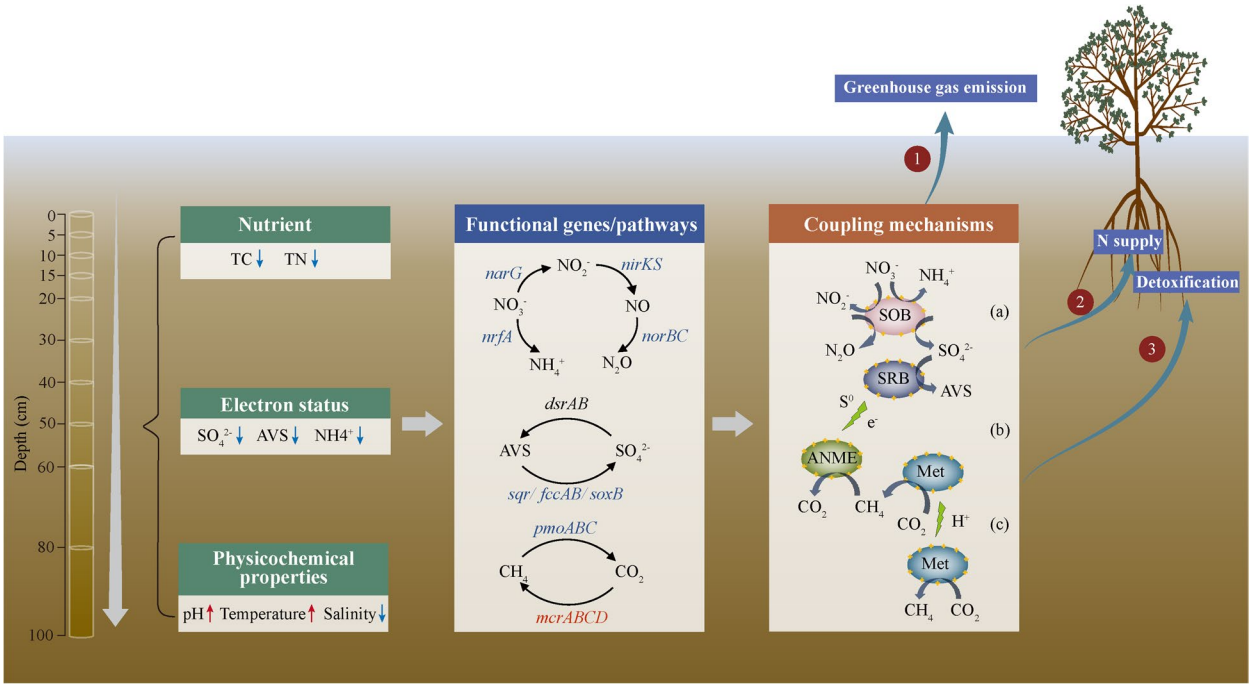

Fig. 7 A conceptual model of depth-related microbially driven CH_4, N and S cycling and their coupling mechanisms in the mangrove sediment. First, physicochemical properties differed vertically by depths and these changes, especially AVS and pH, had a great effect on the distribution of functional genes/pathways involved in CH_4, N and S cycling. Second, possible coupling mechanisms were proposed: a SOB-denitrifier/DNRA; b SRB-methanogen; c Methanogen-methanogen. The relative abundance of functional genes involved in denitrification and S oxidation was enriched in the surface sediment and they could be coupled by S-driven autotrophic denitrifiers, such as *Burkholderiaceae* and *Sulfurifustis*, whereas those involved in dissimilatory sulphate reduction and methanogenesis were enriched in the middle and deep sediments. SRB could co-exist with methanogens in the middle sediment, which could be pulled forward upon the demand of ANME and SOB or directly transfer H^+ or electrons. Third, the depth-related CH_4, N and S cycling microbiomes and their coupling processes may have a great effect on mangrove ecosystem functions and services, such as greenhouse gas emissions, N supply for plant growth, and detoxification. The red and blue colours of words and arrows represent increase or decrease of environmental variables or key genes, respectively along the sediment depth. Black-coloured genes indicate no momentous differences along the sediment depth. Yellow arrows represent H^+/e^- transfer between microbes. TC: total carbon; TN: total nitrogen; AVS: acid volatile sulphide; SOB: sulphur oxidizer; SRB: sulphate reducer; ANME: anaerobic methane oxidizer; Met: methanogen

associated microorganisms with AVS as an important electron donor [123]. Together, our study indicated that environmental factors especially pH and AVS made great contributions to shaping the vertically stratified CH_4, N, and S cycling processes, among which, AVS was a critical electron donor impacting mangrove sediment S oxidation and denitrification. High abundances of gene families involved in S oxidation and denitrification were distributed in the surface sediment and coupled by S-oxidizing denitrifers, while SRB could flexibly interact with methanogens possibly by AOM in the middle layer, indicating the important role of S cycling microbes in microbial interactions and functions in mangrove ecosystems.

Conclusions

Our metagenome sequencing analysis unveiled vertically stratified CH_4, N and S cycling microbiomes and their coupling mechanisms in the mangrove sediment (Fig. 7). The results showed distinct variations of CH_4, N and S cycling genes/pathways mainly driven by pH and AVS along the sediment depth, and S cycling microbes could play key roles in coupling important biogeochemical processes, such as S oxidation and denitrification, methanogenesis and sulphate reduction, and anaerobic methane oxidation and sulphate reduction. S oxidation coupled with denitrification was found to be dominant in the surface sediment, while SRB might develop syntrophic relationships with ANME by direct electron transfer or zero-valent sulphur, and pull forward the co-existence of methanogens and SRB in the middle and deep sediments. The coupling of those biogeochemical processes may ensure the metabolic versatility of CH_4, N and S cycling microbiomes, maintaining mangrove ecosystem functions and services, such as detoxification, N supply for plant growth and greenhouse gas emissions. This study provides new insights into a comprehensive understanding of microbially driven CH_4, N, and S cycling genes/pathways and possible coupling mechanisms along the sediment depth in mangrove ecosystems. Future studies are needed to clarify ecological and molecular mechanisms of energy and matter transfers involved in each of metabolic pathways to depict a full picture of tightly coupled biogeochemical processes in mangrove sediments.

Abbreviations

ANME	Anaerobic CH_4 oxidizer
ANOSIM	Analysis of similarity
ANOVA	Analysis of variance
AOM	Anaerobic oxidation of methane
AVS	Acid volatile sulphide
C	Carbon
CH_4	Methane
MAG	Metagenome-assembled genome
MENA	Molecular ecological network analysis
MIC	Maximal information coefficient
MRPP	Multiple response permutation procedure
N	Nitrogen
ORF	Open reading frame
PCoA	Principal coordinates analysis
S	Sulphur
SDS	Sodium dodecyl sulphate
SOB	s-oxidizing bacteria
SRB	Sulphate-reducing bacteria
TC	Total carbon
TN	Total nitrogen
TPM	Transcripts per million
TS	Total sulphur

Supplementary Information

The online version contains supplementary material available at https://doi.org/10.1186/s40168-023-01501-5.

Additional file 1: Table S1. Summary of sequence information of different samples in each step of metagenome sequencing analysis. **Table S2.** Multiple response permutation procedure (MRPP) analysis of functional profiles related to methane, nitrogen and sulphur cycling among different depths. **Table S3.** Analysis of similarity (ANOSIM) based on functional profiles related to methane, nitrogen and sulphur cycling among different depths. **Table S4.** The vertical distribution of physicochemical characteristics of all mangrove sediment samples in this study. **Table S5.** Summary statistics for Mantel tests of correlations between metabolic pathways and environmental factors. **Table S6.** Summary of correlations between functional groups and keystones. **Table S7.** Summary of correlations between functional groups in the deep sediment. **Fig. S1.** The location of the sampling site at the Qi'ao Mangrove Reserve, Zhuhai, Guangdong province, China. **Fig. S2.** The depth-dependent profile of community structure in mangrove sediments (a) and linear regression analysis of correlations between the relative abundance of *Proteobacteria* and *Euryarchaeota* (b). **Fig. S3.** Principal coordinate analysis (PCoA) plot of all microbial functions (a), methane cycling (b), nitrogen cycling (c), and sulphur cycling (d). **Fig. S4.** Principal coordinate analysis (PCoA) plot of all microbial communities (a), and CH_4-cycling (b), N-cycling (c) and S-cycling (d) microbial communities. **Fig. S5.** A heatmap plot of functional pathways for predicted open reading frames (ORFs) from metagenome sequence reads for sediment samples at different depths. **Fig. S6.** The vertical distribution of relative abundances of key gene families involved in methane cycling. **Fig. S7.** The vertical distribution of relative abundances of key gene families involved in nitrogen cycling. **Fig. S8.** The vertical distribution of the relative abundance of key microbial taxa (top 5) responsible for genes involved in S oxidation and denitrification. **Fig. S9.** The vertical distribution of relative abundances of key gene families involved in sulphur cycling. **Fig. S10.** Correlations between the relative abundance of key gene families. **Fig. S11.** Methane, nitrogen and sulphur cycling co-occurrence networks of three sediment layers at the species level with OTUs colored by phylum/class. **Fig. S12.** The vertical distribution of relative abundances of retrieved methanogen/ANME/SRB MAGs. **Fig. S13.** Metabolic profiles of retrieved MAGs (A) and relative abundances of selected MAGs (B). **Fig. S14.** Carbon, nitrogen, sulphur and metal metabolisms involved in different selected lineages.

Additional file 2: Dataset S1. Genomic information of high quality bins. **Dataset S2.** METABOLIC HMM hits in MAGs. **Dataset S3.** Desulfurivibrionaceae (KO6.bin.24) metabolism. "+" = gene present in the MAG. "Absent" = not present in the MAG. **Dataset S4.** Methanoperedens (KO6.bin.60) metabolism. "+" = gene present in the MAG. "Absent" = not present in the MAG.

Authors' contributions

L.Q., X.L.Y. and Z.L.H. conceived and designed the study. L.Q., H.G., F.L. and C.W. performed sampling and laboratory experiments. L.Q., X.L.Y., Y.J.F. and F.L. carried out the bioinformatics and statistical analysis. L.Q. wrote the first draft of the manuscript. Q.H., L.F.S., S.Q.W., Q.Y.Y, J.G.H, G.L.L, Q.C.T., Z.J.H and Z.L.H.

discussed results and edited the paper. All authors read and approved the final version of the manuscript.

Funding
This work was supported by the National Natural Science Foundation of China (91951207, 92251306, 31971446, 92051110 and 32100077), the Program of Department of Natural Resources of Guangdong Province (GDNRC[2021]62), Southern Marine Science and Engineering Guangdong Laboratory (Zhuhai) (SML2020SP004), China Postdoctoral Science Foundation (2021M703751) and by Sun Yat-Sen University, China.

Availability of data and materials
The metagenomic data of microbial communities in mangrove sediments were deposited in National Omics Data Encyclopedia (NODE) under accession number OEX012906. The authors declare that the primary data supporting the findings of this study are available within this article and in the additional files. Extra data supporting the findings of this study are available from the corresponding authors upon request.

Declarations

Ethics approval and consent to participate
This manuscript does not report data collected from humans or animals. Therefore, ethics approval and a consent to participate are not necessary.

Consent for publication
Not applicable.

Competing interests
The authors declare that they have no competing interests.

Author details
[1]Environmental Microbiomics Research Center, School of Environmental Science and Engineering, Southern Marine Science and Engineering Guangdong Laboratory (Zhuhai), State Key Laboratory of Biocontrol, Sun Yat-Sen University, Guangzhou 510006, China. [2]Department of Civil and Environmental Engineering, the University of Tennessee, Knoxville, TN 37996, USA. [3]Key Laboratory of the Ministry of Education for Coastal and Wetland Ecosystems, School of Life Sciences, Xiamen University, Xiamen 361005, China. [4]School of Marine Science, Sun Yat-Sen University, Zhuhai 519080, China. [5]School of Life Science, Sun Yat-Sen University, Guangzhou 510275, China. [6]Institute of Marine Science and Technology, Shandong University, Qingdao 266237, China.

Received: 13 September 2022 Accepted: 20 February 2023
Published online: 05 April 2023

References

1. Al-Haj AN, Fulweiler RW. A synthesis of methane emissions from shallow vegetated coastal ecosystems. Glob Chang Biol. 2020;26(5):2988–3005.
2. Myllykangas J-P, Rissanen AJ, Hietanen S, Jilbert T. Influence of electron acceptor availability and microbial community structure on sedimentary methane oxidation in a boreal estuary. Biogeochemistry. 2020;148(3):291–309.
3. Neina D. The role of soil pH in plant nutrition and soil remediation. Appl Environ Soil Sci. 2019;2019:5794869.
4. Handley KM, VerBerkmoes NC, Steefel CI, Williams KH, Sharon I, Miller CS, et al. Biostimulation induces syntrophic interactions that impact C, S and N cycling in a sediment microbial community. ISME J. 2013;7(4):800–16.
5. Thatoi H, Behera BC, Mishra RR, Dutta SK. Biodiversity and biotechnological potential of microorganisms from mangrove ecosystems: a review. Ann Microbiol. 2012;63(1):1–19.
6. Yu X, Yang X, Wu Y, Peng Y, Yang T, Xiao F, et al. *Sonneratia apetala* introduction alters methane cycling microbial communities and increases methane emissions in mangrove ecosystems. Soil Biol Biochem. 2020;144:107775.
7. Gao CH, Zhang S, Ding QS, Wei MY, Li H, Li J, et al. Source or sink? A study on the methane flux from mangroves stems in Zhangjiang estuary, southeast coast of China. Sci Total Environ. 2021;788:147782.
8. Jordan SJ, Stoffer J, Nestlerode JA. Wetlands as sinks for reactive nitrogen at continental and global scales: a meta-analysis. Ecosystems. 2010;14(1):144–55.
9. Reis CRG, Nardoto GB, Oliveira RS. Global overview on nitrogen dynamics in mangroves and consequences of increasing nitrogen availability for these systems. Plant Soil. 2016;410:1–19.
10. SamKamaleson A, Gonsalves M-J. Role of sulfur-oxidizing bacteria on the ecology in tropical mangrove sediments. Reg Stud Mar Sci. 2019;28:100574.
11. Nobrega MS, Silva BS, Tschoeke DA, Appolinario LR, Calegario G, Venas TM, et al. Mangrove microbiome reveals importance of sulfur metabolism in tropical coastal waters. Sci Total Environ. 2021;813:151889.
12. Alongi DM. Carbon cycling and storage in mangrove forests. Annu Rev Mar Sci. 2014;6:195–219.
13. Zhang M, Dai P, Lin X, Lin L, Hetharua B, Zhang Y, et al. Nitrogen loss by anaerobic ammonium oxidation in a mangrove wetland of the Zhangjiang Estuary, China. Sci Total Environ. 2020;698:134291.
14. Shen L-d, Liu S, He Z-f, Lian X, Huang Q, He Y-f, et al. Depth-specific distribution and importance of nitrite-dependent anaerobic ammonium and methane-oxidising bacteria in an urban wetland. Soil Biol Biochem. 2015;83:43–51.
15. Jiao S, Chen W, Wang J, Du N, Li Q, Wei G. Soil microbiomes with distinct assemblies through vertical soil profiles drive the cycling of multiple nutrients in reforested ecosystems. Microbiome. 2018;6(1):146.
16. Wu J, Hong Y, Liu X, Hu Y. Variations in nitrogen removal rates and microbial communities over sediment depth in Daya Bay, China. Environ Pollut. 2021;286:117267.
17. Gao H, Schreiber F, Collins G, Jensen MM, Svitlica O, Kostka JE, et al. Aerobic denitrification in permeable Wadden Sea sediments. ISME J. 2010;4(3):417–26.
18. Vandieken V, Finke N, Thamdrup B. Hydrogen, acetate, and lactate as electron donors for microbial manganese reduction in a manganese-rich coastal marine sediment. FEMS Microbiol Ecol. 2014;87(3):733–45.
19. Behera B, Mishra R, Dutta S, Thatoi H. Sulphur oxidising bacteria in mangrove ecosystem: a review. Afr J Biotechnol. 2014;13(29):2897–907.
20. Lin X, Hetharua B, Lin L, Xu H, Zheng T, He Z, et al. Mangrove sediment microbiome: adaptive microbial assemblages and their routed biogeochemical processes in Yunxiao Mangrove National Nature Reserve. China Microb Ecol. 2019;78(1):57–69.
21. Zhang K, Wu X, Wang W, Chen J, Luo H, Chen W, et al. Anaerobic oxidation of methane (AOM) driven by multiple electron acceptors in constructed wetland and the related mechanisms of carbon, nitrogen, sulfur cycles. Chem Eng J. 2022;433:133663.
22. Wang Q, Rogers MJ, Ng SS, He J. Fixed nitrogen removal mechanisms associated with sulfur cycling in tropical wetlands. Water Res. 2021;189:116619.
23. Luo Z, Zhong Q, Han X, Hu R, Liu X, Xu W, et al. Depth-dependent variability of biological nitrogen fixation and diazotrophic communities in mangrove sediments. Microbiome. 2021;9(1):212.
24. Sheng N, Wu F, Liao B, Xin K. Methane and carbon dioxide emissions from cultivated and native mangrove species in Dongzhai Harbor, Hainan. Ecol Eng. 2021;168:106285.
25. Walker CB, Redding-Johanson AM, Baidoo EE, Rajeev L, He Z, Hendrickson EL, et al. Functional responses of methanogenic archaea to syntrophic growth. ISME J. 2012;6(11):2045–55.
26. Llorens-Mares T, Yooseph S, Goll J, Hoffman J, Vila-Costa M, Borrego CM, et al. Connecting biodiversity and potential functional role in modern euxinic environments by microbial metagenomics. ISME J. 2015;9(7):1648–61.
27. Liao W, Tong D, Li Z, Nie X, Liu Y, Ran F, et al. Characteristics of microbial community composition and its relationship with carbon, nitrogen and sulfur in sediments. Sci Total Environ. 2021;795:148848.
28. Marzocchi U, Trojan D, Larsen S, Meyer RL, Revsbech NP, Schramm A, et al. Electric coupling between distant nitrate reduction and sulfide oxidation in marine sediment. ISME J. 2014;8(8):1682–90.

29. Boetius A, Ravenschlag K, Schubert CJ, Rickert D, Widdel F, Gieseke A, et al. A marine microbial consortium apparently mediating anaerobic oxidation of methane. Nature. 2000;407(6804):623–6.
30. Skirnisdottir S, Hreggvidsson GO, Holst O, Kristjansson JK. Isolation and characterization of a mixotrophic sulfur-oxidizing *Thermus scotoductus*. Extremophiles. 2001;5(1):45–51.
31. Milucka J, Ferdelman TG, Polerecky L, Franzke D, Wegener G, Schmid M, et al. Zero-valent sulphur is a key intermediate in marine methane oxidation. Nature. 2012;491(7425):541–6.
32. Sun W, Sun X, Li B, Xu R, Young LY, Dong Y, et al. Bacterial response to sharp geochemical gradients caused by acid mine drainage intrusion in a terrace: relevance of C, N, and S cycling and metal resistance. Environ Int. 2020;138:105601.
33. Li M, Fang A, Yu X, Zhang K, He Z, Wang C, et al. Microbially-driven sulfur cycling microbial communities in different mangrove sediments. Chemosphere. 2021;273:128597.
34. Plugge CM, Zhang W, Scholten JC, Stams AJ. Metabolic flexibility of sulfate-reducing bacteria. Front Microbiol. 2011;2:81.
35. Overmann J, Gemerden H. Microbial interactions involving sulfur bacteria: implications for the ecology and evolution of bacterial communities. FEMS Microbiol Rev. 2000;24(5):591–9.
36. Hsieh YP, Shieh YN. Analysis of reduced inorganic sulfur by diffusion methods: improved apparatus and evaluation for sulfur isotopic studies. Chem Geol. 1997;137(3):255–61.
37. Zhou J, Bruns MA, Tiedje JM. DNA recovery from soils of diverse composition. Appl Environ Microbiol. 1996;62(2):316–22.
38. Yan L, Yang M, Guo H, Yang L, Wu J, Li R, et al. Single-cell RNA-Seq profiling of human preimplantation embryos and embryonic stem cells. Nat Struct Mol Biol. 2013;20(9):1131–9.
39. Zhang J, Kobert K, Flouri T, Stamatakis A. PEAR: a fast and accurate Illumina Paired-End reAd mergeR. Bioinformatics. 2014;30(5):614–20.
40. Qian L, Yu X, Zhou J, Gu H, Ding J, Peng Y, et al. MCycDB: a curated database for comprehensively profiling methane cycling processes of environmental microbiomes. Mol Ecol Resour. 2022;22(5):1803–23.
41. Yu X, Zhou J, Song W, Xu M, He Q, Peng Y, et al. SCycDB: a curated functional gene database for metagenomic profiling of sulphur cycling pathways. Mol Ecol Resour. 2021;21(3):924–40.
42. Tu Q, Lin L, Cheng L, Deng Y, He Z. NCycDB: a curated integrative database for fast and accurate metagenomic profiling of nitrogen cycling genes. Bioinformatics. 2019;35(6):1040–8.
43. Buchfink B, Xie C, Huson DH. Fast and sensitive protein alignment using DIAMOND. Nat Methods. 2015;12(1):59–60.
44. Wood DE, Lu J, Langmead B. Improved metagenomic analysis with Kraken 2. Genome Biol. 2019;20(1):257.
45. Shen W, Le S, Li Y, Hu F. SeqKit: a cross-platform and ultrafast toolkit for FASTA/Q file manipulation. PLoS One. 2016;11(10):e0163962.
46. Li D, Liu C-M, Luo R, Sadakane K, Lam T-W. MEGAHIT: an ultra-fast single-node solution for large and complex metagenomics assembly via succinct de Bruijn graph. Bioinformatics. 2015;31(10):1674–6.
47. Patro R, Duggal G, Love MI, Irizarry RA, Kingsford C. Salmon provides fast and bias-aware quantification of transcript expression. Nat Methods. 2017;14(4):417–9.
48. Kang DD, Li F, Kirton E, Thomas A, Egan R, An H, et al. MetaBAT 2: an adaptive binning algorithm for robust and efficient genome reconstruction from metagenome assemblies. PeerJ. 2019;7:e7359.
49. Olm MR, Brown CT, Brooks B, Banfield JF. dRep: a tool for fast and accurate genomic comparisons that enables improved genome recovery from metagenomes through de-replication. ISME J. 2017;11(12):2864–8.
50. Parks DH, Imelfort M, Skennerton CT, Hugenholtz P, Tyson GW. CheckM: assessing the quality of microbial genomes recovered from isolates, single cells, and metagenomes. Genome Res. 2015;25(7):1043–55.
51. Parks DH, Rinke C, Chuvochina M, Chaumeil P-A, Woodcroft BJ, Evans PN, et al. Recovery of nearly 8,000 metagenome-assembled genomes substantially expands the tree of life. Nat Microbiol. 2017;2(11):1533–42.
52. Johnston ER, Hatt JK, He Z, Wu L, Guo X, Luo Y, et al. Responses of tundra soil microbial communities to half a decade of experimental warming at two critical depths. Proc Natl Acad Sci U S A. 2019;116(30):15096–105.
53. Chaumeil PA, Mussig AJ, Hugenholtz P, Parks DH. GTDB-Tk: a toolkit to classify genomes with the Genome Taxonomy Database. Bioinformatics. 2019;36(6):1925–7.
54. Zhou Z, Tran PQ, Breister AM, Liu Y, Kieft K, Cowley ES, et al. METABOLIC: high-throughput profiling of microbial genomes for functional traits, metabolism, biogeochemistry, and community-scale functional networks. Microbiome. 2022;10(1):33.
55. Cantalapiedra CP, Hernández-Plaza A, Letunic I, Bork P, Huerta-Cepas J. eggNOG-mapper v2: Functional Annotation, Orthology Assignments, and Domain Prediction at the Metagenomic Scale. Mol Biol Evol. 2021;38(12):5825–9.
56. Deng Y, Jiang Y-H, Yang Y, He Z, Luo F, Zhou J. Molecular ecological network analyses. BMC Bioinform. 2012;13(1):113.
57. Shannon P, Markiel A, Ozier O, Baliga NS, Wang JT, Ramage D, et al. Cytoscape: a software environment for integrated models of biomolecular interaction networks. Genome Res. 2003;13(11):2498–504.
58. Reshef David N, Reshef Yakir A, Finucane Hilary K, Grossman Sharon R, McVean G, Turnbaugh Peter J, et al. Detecting novel associations in large data sets. Science. 2011;334(6062):1518–24.
59. Albanese D, Filosi M, Visintainer R, Riccadonna S, Jurman G, Furlanello C. Minerva and minepy: a C engine for the MINE suite and its R, Python and MATLAB wrappers. Bioinformatics. 2013;29:407–8.
60. Wickham H. Reshaping Data with the reshape Package. J Stat Softw. 2007;21:1–20.
61. Kassambara A. rstatix: pipe-friendly framework for basic statistical tests. R package version 0.6.0; 2020.
62. Oksanen J, Simpson GL, Blanchet FG, Kindt R, Legendre P, Minchin PR, et al. vegan: Community Ecology Package. R package 2.6. 2022.
63. Wickham H. ggplot2: elegant graphics for data analysis. New York: Springer; 2016.
64. Kolde R. pheatmap: Pretty Heatmaps. R Package Version 1.0.12; 2019.
65. Maher DT, Call M, Santos IR, Sanders CJ. Beyond burial: lateral exchange is a significant atmospheric carbon sink in mangrove forests. Biol Lett. 2018;14(7):20180200.
66. Zeleke J, Lu S-L, Wang J-G, Huang J-X, Li B, Ogram AV, et al. Methyl coenzyme M reductase A (*mcrA*) gene-based investigation of methanogens in the mudflat sediments of Yangtze River Estuary, China. Microb Ecol. 2013;66(2):257–67.
67. Carr SA, Schubotz F, Dunbar RB, Mills CT, Dias R, Summons RE, et al. Acetoclastic Methanosaeta are dominant methanogens in organic-rich Antarctic marine sediments. ISME J. 2018;12(2):330–42.
68. Katayama T, Yoshioka H, Kaneko M, Amo M, Fujii T, Takahashi HA, et al. Cultivation and biogeochemical analyses reveal insights into methanogenesis in deep subseafloor sediment at a biogenic gas hydrate site. ISME J. 2022;16(5):1464–72.
69. Horn MA, Matthies C, Küsel K, Schramm A, Drake HL. Hydrogenotrophic methanogenesis by moderately acid-tolerant methanogens of a methane-emitting acidic peat. Appl Environ Microbiol. 2003;69(1):74–83.
70. Zhang C-J, Pan J, Liu Y, Duan C-H, Li M. Genomic and transcriptomic insights into methanogenesis potential of novel methanogens from mangrove sediments. Microbiome. 2020;8(1):94.
71. Liu D, Ding W, Jia Z, Cai Z. The impact of dissolved organic carbon on the spatial variability of methanogenic archaea communities in natural wetland ecosystems across China. Appl Microbiol Biotechnol. 2012;96(1):253–63.
72. Bräuer S, Cadillo-Quiroz H, Kyrpides N, Woyke T, Goodwin L, Detter C, et al. Genome of *Methanoregula boonei* 6A8 reveals adaptations to oligotrophic peatland environments. Microbiology. 2015;161(8):1572–81.
73. Sakai S, Imachi H, Sekiguchi Y, Tseng I-C, Ohashi A, Harada H, et al. Cultivation of methanogens under low-hydrogen conditions by using the coculture method. Appl Environ Microbiol. 2009;75(14):4892–6.
74. Li D, Ni H, Jiao S, Lu Y, Zhou J, Sun B, et al. Coexistence patterns of soil methanogens are closely tied to methane generation and community assembly in rice paddies. Microbiome. 2021;9(1):20.
75. Zhuang W, Yu X, Hu R, Luo Z, Liu X, Zheng X, et al. Diversity, function and assembly of mangrove root-associated microbial communities at a continuous fine-scale. Npj Biofilms Microbi. 2020;6(1):52.
76. Håvelsrud OE, Haverkamp THA, Kristensen T, Jakobsen KS, Rike AG. A metagenomic study of methanotrophic microorganisms in Coal Oil Point seep sediments. BMC Microbiol. 2011;11(1):221.
77. Shen L-d, Wu H-s, Liu X, Li J. Vertical distribution and activity of anaerobic ammonium-oxidising bacteria in a vegetable field. Geoderma. 2017;288:56–63.

78. Fernandes SO, Bonin PC, Michotey VD, Garcia N, LokaBharathi PA. Nitrogen-limited mangrove ecosystems conserve N through dissimilatory nitrate reduction to ammonium. Sci Rep. 2012;2:419.
79. Bateman EJ, Baggs EM. Contributions of nitrification and denitrification to N_2O emissions from soils at different water-filled pore space. Biol Fertil Soils. 2005;41(6):379–88.
80. Xu X, Ouyang H, Richter A, Wanek W, Cao G, Kuzyakov Y. Spatio-temporal variations determine plant-microbe competition for inorganic nitrogen in an alpine meadow. J Ecol. 2011;99:563–71.
81. Qin DU, Lifeng LI. Temporal-spatial distribution features in the root system of individual *Sonneratia apetala* and *Avicennia marina* plants. Acta Ecol Sin. 2018;38(17):6055–62.
82. An S, Gardner WS. Dissimilatory nitrate reduction to ammonium (DNRA) as a nitrogen link, versus denitrification as a sink in a shallow estuary (Laguna Madre/Baffin Bay, Texas). Mar Ecol Prog Ser. 2002;237:41–50.
83. Cao W, Yang J, Li Y, Liu B, Wang F, Chang C. Dissimilatory nitrate reduction to ammonium conserves nitrogen in anthropogenically affected subtropical mangrove sediments in Southeast China. Mar Pollut Bull. 2016;110(1):155–61.
84. Leloup J, Loy A, Knab NJ, Borowski C, Wagner M, Jorgensen BB. Diversity and abundance of sulfate-reducing microorganisms in the sulfate and methane zones of a marine sediment, Black Sea. Environ Microbiol. 2007;9(1):131–42.
85. Dalcin Martins P, Hoyt DW, Bansal S, Mills CT, Tfaily M, Tangen BA, et al. Abundant carbon substrates drive extremely high sulfate reduction rates and methane fluxes in Prairie Pothole Wetlands. Glob Chang Biol. 2017;23(8):3107–20.
86. Pi N, Tam NF, Wong MH. Effects of wastewater discharge on formation of Fe plaque on root surface and radial oxygen loss of mangrove roots. Environ Pollut. 2010;158(2):381–7.
87. Loy A, Duller S, Baranyi C, Mußmann M, Ott J, Sharon I, et al. Reverse dissimilatory sulfite reductase as phylogenetic marker for a subgroup of sulfur-oxidizing prokaryotes. Environ Microbiol. 2009;11(2):289–99.
88. Großkopf T, Soyer OS. Microbial diversity arising from thermodynamic constraints. ISME J. 2016;10(11):2725–33.
89. Shao MF, Zhang T, Fang HH. Sulfur-driven autotrophic denitrification: diversity, biochemistry, and engineering applications. Appl Microbiol Biotechnol. 2010;88(5):1027–42.
90. Grote J, Schott T, Bruckner C, Glöckner F, Jost G, Teeling H, et al. Genome and physiology of a model Epsilonproteobacterium responsible for sulfide detoxification in marine oxygen depletion zones. Proc Natl Acad Sci U S A. 2011;109:506–10.
91. Berben T, Overmars L, Sorokin DY, Muyzer G. Diversity and distribution of sulfur oxidation-related genes in *Thioalkalivibrio*, a genus of chemolithoautotrophic and haloalkaliphilic sulfur-oxidizing bacteria. Front Microbiol. 2019;10:160.
92. Allen DE, Dalal RC, Rennenberg H, Meyer RL, Reeves S, Schmidt S. Spatial and temporal variation of nitrous oxide and methane flux between subtropical mangrove sediments and the atmosphere. Soil Biol Biochem. 2007;39(2):622–31.
93. Rosentreter JA, Al-Haj AN, Fulweiler RW, Williamson P. Methane and nitrous oxide emissions complicate coastal blue carbon assessments. Global Biogeochem Cy. 2021;35(2):e2020GB006858.
94. Fernandes SO, Bharathi PAL, Bonin PC, Michotey VD. Denitrification: an important pathway for nitrous oxide production in tropical mangrove sediments (Goa, India). J Environ Qual. 2010;39(4):1507–16.
95. Volland J-M, Gonzalez-Rizzo S, Gros O, Tyml T, Ivanova N, Schulz F, et al. A centimeter-long bacterium with DNA contained in metabolically active, membrane-bound organelles. Science. 2022;376(6600):1453–8.
96. Levin PA. A bacterium that is not a microbe. Science. 2022;376(6600):1379–80.
97. Chen Z, Zhong X, Zheng M, Liu W-S, Fei Y, Ding K, et al. Indicator species drive the key ecological functions of microbiota in a river impacted by acid mine drainage generated by rare earth elements mining in South China. Environ Microbiol. 2022;24(2):919–37.
98. Janssen PJ, Van Houdt R, Moors H, Monsieurs P, Morin N, Michaux A, et al. The complete genome sequence of *Cupriavidus metallidurans* strain CH34, a master survivalist in harsh and anthropogenic environments. PLoS One. 2010;5(5):e10433.
99. Kojima H, Shinohara A, Fukui M. *Sulfurifustis variabilis* gen. nov., sp. nov., a sulfur oxidizer isolated from a lake, and proposal of Acidiferrobacteraceae fam. nov. and Acidiferrobacterales ord. nov. Int J Syst Evol Microbiol. 2015;65(10):3709–13.
100. Plummer P, Tobias C, Cady D. Nitrogen reduction pathways in estuarine sediments: influences of organic carbon and sulfide. J Geophys Res-Biogeo. 2015;120(10):1958–72.
101. Zhu J, He Y, Zhu Y, Huang M, Zhang Y. Biogeochemical sulfur cycling coupling with dissimilatory nitrate reduction processes in freshwater sediments. Environ Rev. 2018;26(2):121–32.
102. Giweta M, Dyck M, Malhi SS, Puurveen D, Quideau SA. Soil nitrous oxide emissions most sensitive to fertilization history during a laboratory incubation. Can J Soil Sci. 2020;100(4):479–87.
103. Oremland RS, Taylor BF. Sulfate reduction and methanogenesis in marine sediments. Geochim Cosmochim Ac. 1978;42(2):209–14.
104. Oremland RS, Marsh LM, Polcin S. Methane production and simultaneous sulphate reduction in anoxic, salt marsh sediments. Nature. 1982;296(5853):143–5.
105. Lyimo TJ, Pol A, Op den Camp HJM. Sulfate reduction and methanogenesis in sediments of Mtoni mangrove forest, Tanzania. Ambio. 2002;31(7):614–6.
106. Lovley DR, Klug MJ. Sulfate reducers can outcompete methanogens at freshwater sulfate concentrations. Appl Environ Microbiol. 1983;45(1):187–92.
107. Sela-Adler M, Ronen Z, Herut B, Antler G, Vigderovich H, Eckert W, et al. Co-existence of methanogenesis and sulfate reduction with common substrates in sulfate-rich estuarine sediments. Front Microbiol. 2017;8:766.
108. Taketani RG, Yoshiura CA, Dias AC, Andreote FD, Tsai SM. Diversity and identification of methanogenic archaea and sulphate-reducing bacteria in sediments from a pristine tropical mangrove. Antonie Van Leeuwenhoek. 2010;97(4):401–11.
109. Lau MC, Kieft TL, Kuloyo O, Linage-Alvarez B, van Heerden E, Lindsay MR, et al. An oligotrophic deep-subsurface community dependent on syntrophy is dominated by sulfur-driven autotrophic denitrifiers. Proc Natl Acad Sci U S A. 2016;113(49):E7927–36.
110. Ino K, Hernsdorf AW, Konno U, Kouduka M, Yanagawa K, Kato S, et al. Ecological and genomic profiling of anaerobic methane-oxidizing archaea in a deep granitic environment. ISME J. 2018;12(1):31–47.
111. Shimoyama T, Kato S, Ishii S, Watanabe K. Flagellum mediates symbiosis. Science. 2009;323(5921):1574.
112. Leu Andy O, McIlroy Simon J, Ye J, Parks Donovan H, Orphan Victoria J, Tyson GW. Lateral gene transfer drives metabolic flexibility in the anaerobic methane-oxidizing archaeal family *Methanoperedenaceae*. mBio. 2020;11(3):e01325–0.
113. Fang W, Liang Z, Liu Y, Liao J, Wang S. Metagenomic insights into production of zero valent sulfur from dissimilatory sulfate reduction in a methanogenic bioreactor. Bioresour Technol Rep. 2019;8:100305.
114. Yang X, Yu X, He Q, Deng T, Guan X, Lian Y, et al. Niche differentiation among comammox (*Nitrospira inopinata*) and other metabolically distinct nitrifiers. Front Microbiol. 2022;13:956860.
115. Fierer N. Embracing the unknown: disentangling the complexities of the soil microbiome. Nat Rev Microbiol. 2017;15(10):579–90.
116. Tripathi BM, Stegen JC, Kim M, Dong K, Adams JM, Lee YK. Soil pH mediates the balance between stochastic and deterministic assembly of bacteria. ISME J. 2018;12(4):1072–83.
117. Zhang J, Jiao S, Lu Y. Biogeographic distribution of bacterial, archaeal and methanogenic communities and their associations with methanogenic capacity in Chinese wetlands. Sci Total Environ. 2018;622-623:664–75.
118. Wen X, Yang S, Horn F, Winkel M, Wagner D, Liebner S. Global biogeographic analysis of methanogenic archaea identifies community-shaping environmental factors of natural environments. Front Microbiol. 2017;8:1339.
119. Schnakenberg A, Aromokeye DA, Kulkarni A, Maier L, Wunder LC, Richter-Heitmann T, et al. Electron acceptor availability shapes anaerobically methane oxidizing archaea (ANME) communities in South Georgia sediments. Front Microbiol. 2021;12:617280.
120. Lee HJ, Kim SY, Kim PJ, Madsen EL, Jeon CO. Methane emission and dynamics of methanotrophic and methanogenic communities in a flooded rice field ecosystem. FEMS Microbiol Ecol. 2014;88(1):195–212.

121. Ye R, Jin Q, Bohannan B, Keller JK, McAllister SA, Bridgham SD. pH controls over anaerobic carbon mineralization, the efficiency of methane production, and methanogenic pathways in peatlands across an ombrotrophic–minerotrophic gradient. Soil Biol Biochem. 2012;54:36–47.
122. Staley BF, de los Reyes FL III, Barlaz MA. Effect of spatial differences in microbial activity, pH, and substrate levels on methanogenesis initiation in refuse. Appl Environ Microbiol. 2011;77(7):2381–91.
123. Šlmek M, Cooper JE. The influence of soil pH on denitrification: progress towards the understanding of this interaction over the last 50 years. Eur J Soil Sci. 2002;53(3):345–54.

Publisher's Note